

# Interpretable Features for the Assessment of Neurodegenerative Diseases through Handwriting Analysis

Thomas Thebaud, *Member, IEEE*, Anna Favaro, *Member, IEEE*, Casey Chen, Gabrielle Chavez, Laureano Moro-Velazquez, *Member, IEEE*, Emile Moukhebeir, Ankur Butala, and Najim Dehak, *Member, IEEE*

**Abstract**—Motor dysfunction is a common sign of neurodegenerative diseases (NDs) such as Parkinson’s disease (PD) and Alzheimer’s disease (AD), but may be difficult to detect, especially in the early stages. In this work, we examine the behavior of a wide array of interpretable features extracted from the handwriting signals of 113 subjects performing multiple tasks on a digital tablet, as part of the Neurological Signals dataset. The aim is to measure their effectiveness in characterizing NDs, including AD and PD. To this end, task-agnostic and task-specific features are extracted from 14 distinct tasks. Subsequently, through statistical analysis and a series of classification experiments, we investigate which features provide greater discriminative power between NDs and healthy controls and amongst different NDs. Preliminary results indicate that the tasks at hand can all be effectively leveraged to distinguish between the considered set of NDs, specifically by measuring the stability, the speed of writing, the time spent not writing, and the pressure variations between groups from our handcrafted interpretable features, which shows a statistically significant difference between groups, across multiple tasks. Using various binary classification algorithms on the computed features, we obtain up to 87% accuracy for the discrimination between AD and healthy controls (CTL), and up to 69% for the discrimination between PD and CTL.

**Index Terms**—Handwriting Analysis, Alzheimer’s Disease, Parkinson’s Disease, Digital Biomarkers, Neurological Signals

## I. INTRODUCTION

Neurodegenerative diseases (NDs), including Parkinson’s disease (PD) and Alzheimer’s disease (AD), progressively impair cognitive, motor, and behavioral functions by affecting both overlapping and distinct brain regions. To monitor these dysfunctions, many studies have explored non-invasive techniques using wearable or digital sensors. Among them, handwriting stands out as a promising modality due to its intricate integration of cognitive, motor, and perceptual processes [1], [2]. Handwriting production recruits a distributed neural network across cortical and subcortical structures, including regions involved in learning, executive function,

praxis, vigilance, and motor coordination—spanning the cerebral cortex, basal ganglia, and cerebellum [3]. Consequently, abnormalities in handwriting patterns can serve as sensitive digital biomarkers of disease presence and progression [4], with micrographia being a well-established early symptom of PD [5].

Both paper-based and digital handwriting tasks have been employed to evaluate ND-related impairments by analyzing the spatial and temporal characteristics of handwriting signals [1], [4], [5]. Historically, most studies have focused on PD, largely due to the overt motor symptoms associated with the disease, including micrographia [6]–[9], tremor [10], and bradykinesia [10]—collectively referred to as PD dysgraphia [1]. Handwriting analysis has also been explored for AD detection [11], as the disease’s prevalence continues to rise [12]–[14].

Numerous handwriting datasets have been introduced to study NDs, capturing either static images or dynamic time-series signals. However, most datasets are restricted to a single disease type and a single data modality, thereby limiting their experimental scope. For the assessment of PD:

- **HandPD** [15]: Includes 92 participants (74 PD, 18 CTL), with image-based recordings of spiral and meander tracing. Naive Bayes classification achieved up to 78.9% accuracy.
- **NewHandPD** [16]: Expanded the previous dataset by adding pressure, acceleration, and tilt data from 14 PD and 21 CTL participants. Using CNNs, the study reached 83.77% accuracy on spirals and 87.14% on meanders.
- **PaHaW** [6]: Collected position and pressure data from spirals and repeated text in 37 PD and 38 CTL subjects. Using interpretable features and SVMs, it achieved 81.3% accuracy.
- **ParkinsonHW** [17]: Recorded dynamic handwriting from 27 PD and 28 CTL subjects via a digital tablet. Cascaded non-neural classifiers achieved 84.67% accuracy on spirals and 90.91% on stability tasks [18].

For the assessment of AD:

- Early work by [14] evaluated handwriting signatures from 29 AD and 30 CTL subjects, achieving a 3% error rate with a decision tree model.
- The dataset introduced by [13] included 23 AD, 12 MCI, and 17 CTL participants performing drawing and writing tasks on a tablet. Sentence copying reached up to 80.4%

Submitted for review: 23/10/2025.

Thomas Thebaud, Anna Favaro, Casey Chen, Gabrielle Chavez, Laureano Moro-Velazquez and Najim Dehak are with the Department of Electrical and Computer Engineering, The Johns Hopkins University, Baltimore MD, USA (e-mail: \*@jhu.edu, \*∈{tthebau1, afavaro1, cchen247, gchavez5, laureano, ndehak3}).

Moukhebeir Emile is with the Department of Neurology, The Johns Hopkins University, Baltimore MD, USA (e-mail: emoukheiber@jhmi.edu).

Butala Ankur is with the Department of Neurology and the Department of Psychiatry and Behavioral Sciences, The Johns Hopkins University, Baltimore MD, USA (e-mail: Ankur.Butala@jhmi.edu).

classification accuracy across three groups.

- **The DARWIN dataset** [12], now a standard benchmark, includes 89 AD and 85 CTL participants engaged in copying, memory, and graphical tasks. Fusing non-neural classifiers trained on individual tasks yielded a top accuracy of 94.29%.

Handwriting tasks for ND assessment can be categorized by complexity and task structure: *Simple motor tasks* involve drawing basic shapes such as spirals or straight lines, or stability exercises, such as maintaining a fixed pen over a tablet. These evaluate tremor, trajectory smoothness, speed, and acceleration [19]. *Written language tasks* involve producing words or sentences. On tablets, these tasks enable the study of in-air movement and motor planning between words [19]. In-air time reflects cognitive preparation [5], and since in-air and on-surface dynamics are non-redundant [20], both provide complementary information. Increased in-air duration may reflect hesitation or planning deficits. *Complex visuoconstructive tasks* include copying figures or drawing clocks. The clock drawing test is an established tool for evaluating visuospatial and executive function across several NDs [21], [22]. Copying tasks allow examination of written response fidelity in varied contexts [23].

In this work, we introduce a new dataset composed of digital handwriting samples from 103 participants, including individuals diagnosed with AD, Mild Cognitive Impairment (MCI), PD, and Related Disorders (a heterogeneous group we refer to as **PDM**, comprising atypical Parkinsonism and misdiagnosed cases). Participants completed 14 tablet-based handwriting tasks specifically designed to probe cognitive and motor deficits across these conditions. We extract a large set of interpretable, quantitative measurements, referred to as handwriting features, from these tasks. These include both: *Task-agnostic features*, which capture global signal properties across all tasks, regardless of their nature, and *Task-specific features*, which target features tailored to particular task types. We then assess which features best distinguish between groups through statistical analyses and binary classification experiments. In particular, we compare ND subgroups (PD, AD, PDM) to healthy controls, and contrast PD and PDM to identify discriminative features within motor phenotypes.

The main contributions of this paper are as follows:

- Introduction of a novel, multi-condition handwriting dataset for ND assessment.
- Inclusion of multiple disease groups, including an active control group (PDM), expanding beyond the narrower focus of prior datasets.
- Extension of handwriting analysis from PD to AD and MCI, which have received limited attention.
- Design and evaluation of a broad set of task-agnostic and task-specific features that align with expected behavioral patterns and reveal significant group differences.
- Novel exploration of inter-task comparisons to analyze behavioral shifts when task parameters change (e.g., drawing hand).

The sections of the manuscripts are organized as follows: Section II presents the data collection pipeline and the main

pre-processing stages. Section III introduces the task-agnostic features extracted from all tasks and the task-specific features designed for specific groups of tasks. Then, various methods used to gauge the significance of our features in the various tasks analyzed are described. Finally, we introduce the methods used for training classifiers for NDs assessment from the presented interpretable features. Section IV shows and discusses our statistical and classification results. Section V contains the main findings, discussions, limits and conclusions of the study.

## II. MATERIALS

In this section, we outline the data collection and pre-processing methods and the tasks evaluated in this research.

### A. Data Collection

The authors of this study collected a dataset from 113 participants from a larger digital biomarker cohort, NeuroLogical Signals, which our group has previously reported [24]–[30]. These participants were either categorized as healthy (CTL) or diagnosed and treated for a ND by a subspecialist neurologist or geriatric psychiatrist from Johns Hopkins Hospital. Participants diagnosed with NDs were categorized into aforementioned groups based on disease specific clinical diagnostic criteria diagnosis:

- AD participants were enrolled from a University AD Center of Excellence, treated by an expert geriatric psychiatrist with an AD diagnosis based upon 2011 criteria [31]. However, most of these subjects were enrolled in serum or CSF biomarker studies confirming their diagnosis reflecting later revisions to diagnostic criteria [32].
- MCI participants were characterized by established criteria, not yet meeting multidomain impairment or disability consistent with AD [33].
- PD participants met international recognized diagnostic criteria at a "clinically established" [34] level of certainty and were followed by a movement disorders neurologist.
- PDM participants presented with one or more core symptoms of PD, meeting a "Probable PD" diagnosis but which was later revised based on evolving characteristics or supportive testing. This is a mixed, active comparator group includes patients later diagnosed with Dementia with Lewy Bodies, Fahr's Disease, Ataxia, Corticobasal Syndrome, Corticobasal Degeneration, Cervical Dystonia, Gerstmann Schenker Schyuler Syndrome, Wilson Disease, MSA-Parkinsonian, and Essential Tremor. In this study, this group is considered an active control group against the PD group.

All participants signed informed consent, and the data collection was approved by the Johns Hopkins Medicine Institutional Review Board. Participants with PD continued their usual pharmacological treatment and took dopaminergic medication before the recording session. Handwriting samples were collected using a Wacom One 13 tablet<sup>1</sup> with the associated pen. This setup enabled us to record the pressure applied by the pen on the tablet surface and its position both on the tablet and in the air when in close proximity. Note the

<sup>1</sup><https://estore.wacom.com/en-us/wacom-one-13-touch-dth134w0a.html>

TABLE I  
DISTRIBUTION OF THE PARTICIPANTS RECORDED IN THE DATASET.

Category	Number of Participants	% Females	Age	Files recorded	MoCA [35]	UPDRS3 [36]
CTL	42	57.1%	69y ( $\pm 11$ )	757	25.4	
PD	35	40.0%	67y ( $\pm 9$ )	608	25.9	24.3
PDM	15	46.7%	53y ( $\pm 14$ )	283	25.8	21.5
AD	21	19.0%	70y ( $\pm 7$ )	745	19.7	
Total	113	43.4%	66y ( $\pm 12$ )	1840		

recording session also included collection of saccadometric and synchronized speech, although these two modalities were not utilized in this study. Participants completed 14 written tasks per session, detailed in Section II-B, guided by a research assistant. We collected recordings for each participant for at least one session, while 21 participants were recorded up to three times, when available and interested, with each session spaced six months apart. The handwriting data collected is part of a larger, multimodal dataset that is yet to be published. The distribution of participants, with their age, gender, and total number of tasks recorded, is presented in Table I. Participants classified as AD and MCI were combined into a single group, named AD\* in this study. Only a subset of the recorded participants were kept in that study, to balance as much as possible the age and gender of the participants. However, given the low number of female participants, gender balancing for the AD\* group was not possible, so we chose to keep the whole group.

### B. Handwriting Tasks

In each session, we collected data from 14 handwriting tasks per participant. Due to myriad reasons, technical or human, the recordings of some tasks can fail, leading to a variable number of participants for each task. Participants having one or more missing tasks are still included in the study. Within this section, we provide a comprehensive description of tasks, their origin (what each of those tasks were used for, initially), and outline the experimental hypotheses we formulated for each. Tasks such as Point and Spiral tasks involved participants performing stability exercises three times: alternating hands, then with their dominant hand while concurrently speaking. **Writing** and **Drawing** tasks prompted participants to replicate an item from the screen, from memory, and generate new content. Participants were asked not to touch the tablet with their arm or hand while writing. Figure 1 illustrates a sample from each task type, encompassing participants from the CTL, AD, PD, and PDM groups.

1) **Point Tasks**: The point tasks are designed to assess the static motor control and stability of the participants. Each participant was asked to maintain the pen vertically above a point shown in the tablet without moving or touching the tablet for 10 sec. More specifically, in the **Point Dominant** and **Point Non-Dominant** tasks, participants are asked to use their dominant and Non-Dominant hand, respectively, and in the **Point Sustained**, they are asked to use their dominant hand, in addition, to sustain the phonation of the vowel A during the exercise.

2) **Spiral Tasks**: The spiral tasks are also designed to assess the dynamic motor control and coordination of the participants.

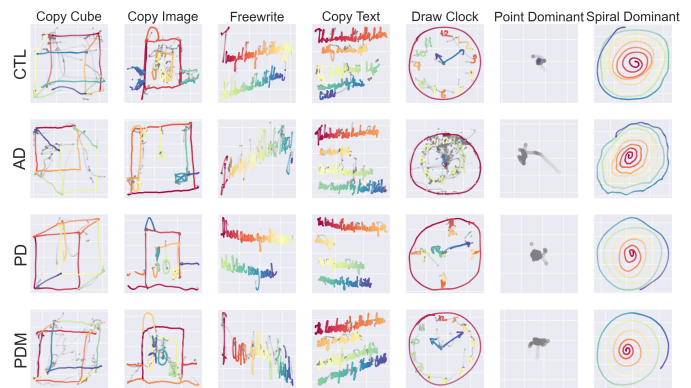


Fig. 1. Example of each type of task from all four experimental groups. When on tablet, the color of the points transits from red to purple. When in air, the points are depicted in gray.

Several clinical rating scales [37], [38] require participants with PD to perform regular circular movement on paper or on tablet to assess their regularity or the presence of an eventual tremor [39]–[41]. The spiral test has also proven useful for AD assessment using a tablet [42]. The participants were asked to draw a spiral starting from the center of the tablet. More specifically, in the **Spiral Dominant** and **Spiral Non-Dominant** tasks, participants were asked to use their dominant and Non-Dominant hand respectively, and in the dual-task **Spiral PaTaKa**, they were asked to use their dominant hand, and simultaneously, to perform a spoken diadochokinetic task, i.e., repeat as fast as possible the syllables *pa*, *ta*, and *ka* in this exact order. However, our current focus lies solely on the handwriting data. We hypothesize that the simultaneous performance of tasks will make it more difficult for participants to use strategies to compensate for the motor impairments caused by NDs.

3) **Writing Tasks**: The writing tasks were designed to assess the cognitive and motor capacities of the participants. Handwriting analysis has been used mostly for the assessment of PD, as some motor symptoms of the disease can be seen through some characteristic modifications of the handwriting, such as micrographia [43], [44]

Participants first engaged in the **Copy Text** task, wherein they were tasked with replicating a paragraph of text displayed on the screen. We then focus on the impact of multitasking by introducing the **Copy Read Text** task, where participants copied another text while simultaneously reading it aloud. Subsequently, participants' spontaneous writing abilities were captured through the **Freewrite** task, prompting them to write freely one or two sentences that must not contain any personal information. Lastly, we exploring handwriting a different context, the **Numbers** task, wherein participants were tasked with solving eight simple arithmetic operations summing two natural numbers not exceeding a total of 20, while saying the results of the sums out loud. It is worth noting that the Numbers task may be analyzed differently from the writing tasks due to its repetitive nature, necessitating a distinct analytical approach.

4) **Drawing Tasks**: The Drawing tasks are also designed to assess the cognitive and visuo-constructive capacities of the

participants.

First, in the **Copy Image** task, we asked participants to copy an image displayed on the screen. The image, is a complex figure in the style of those used in the Complex Figure Task [45]: asymmetric, non-patterned with internal and external details, as shown in the figure 2

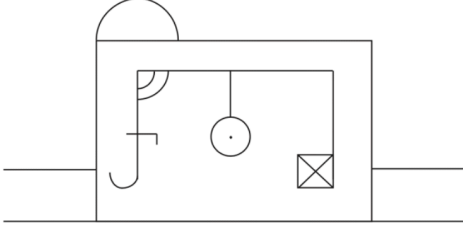


Fig. 2. Target image presented to the participants for the **copy image** and **copy image memory** tasks.

We further examined the impact of memory on this behavior by introducing the **Copy Image Memory** task. After copying the image in the **Copy Image** task, participants were then asked to reproduce it from memory approximately five minutes later, thus assessing visual memory and construction abilities.

Subsequently, participants were asked to perform two tasks: First, the **Draw Clock** task, which looked at their ability to draw all the required elements of a clock at an instructed time [46]. The Clock Draw Task is another established visuo-constructive screen studied in PD [22] and AD [35] which has been utilized to distinguish ND [47] and may be interpreted in a number of ways.

Then, the **Draw Cube** task, used in the MoCA test [35] and which has been proved to be also useful for PD assessment [48], examines their capacity to represent a three-dimensional object.

### C. Data Curation

Every task starts and concludes with a participant crossing an area marked as start or end on the screen, respectively, using a pen. However, the portion of the recording relevant to the analysis is shorter than the entirety captured. Hence, we manually eliminated the empty segments before and after the tasks commenced. Files lacking task-related responses are removed.

## III. METHODS

This section outlines the features calculated for each task and the methods used to assess their significance among different experimental groups. We developed interpretable features from raw handwriting signals collected during various tasks. Our analysis has two aspects: first, we examine dynamic handwriting properties common to all tasks; second, we evaluate performance in specific tasks, such as stability in point tasks and proximity between drawing and target in copying tasks.

### A. Features computation pipeline

To compute the features analyzed in this study, we follow the pipeline described in Figure 3. Each data file can be described as a time series containing  $N \in \mathbb{R}$  points:

- The positions  $X = (x_i)_{i \in [[1, N]]}$  and  $Y = (y_i)_{i \in [[1, N]]}$

- The time stamps  $T = (t_i)_{i \in [[1, N]]}$
- The pressure  $P = (p_i)_{i \in [[1, N]]}$

We define a clean file as the list  $\mathcal{F} = [X_u, Y_u, P_u, T_u]$ .

We computed various features from the clean files, targeting prioritizing motor, cognitive or behavioral elements. The features can be categorized relative to or irrespective of the task:

- 1) Task-agnostic (see Section III-B): these features measure primarily dynamic properties of the signal such as speed, noise, and basic ratios.
- 2) Task-specific (see Section III-C): these features are designed for specific tasks or groups of tasks.

### B. Task-Agnostic Features

Task-agnostic features quantify the dynamic aspects of the drawings. They are computed using several signal-processing techniques. The extraction process, illustrated in Figure 3, may be parsed:

- 1) computation of time series from the raw data, such as the angle between 2 consecutive points, the distance between two points, and multiple derivations (see Section III-B1).
- 2) segmentation of each series using only the segments gathered In-Air or On-Tablet. A stroke being defined as the trajectory On-Tablet between two In-Air moments. The segmentation is described in Section III-B2
- 3) computation of statistics (e.g., mean, the standard deviation) on the time-series obtained from the derivation of *time independent features*, described in Section III-B3.

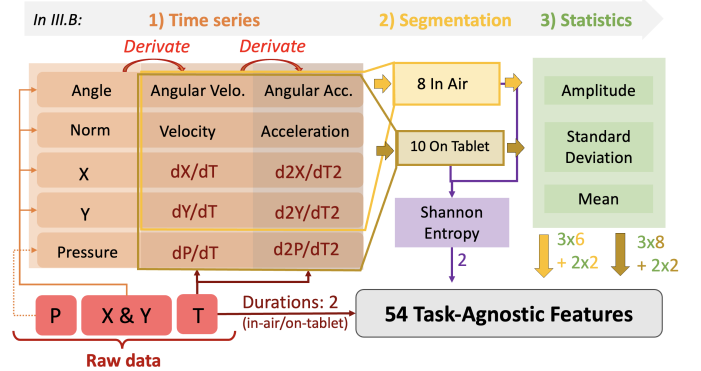


Fig. 3. Pipeline used to extract task-agnostic features across all tasks. From the raw data, 5 time series are extracted, differentiated twice, and then the segmentation selects only the in-air parts (yellow path) or the on-tablet parts (brown path), and statistics and entropy are computed from each segmented time-series. The amplitudes for angular velocity and acceleration are not kept, which is why we have 54 and not 58 features.

1) *Time series*: For every point of a given clean data file, we compute the angle and the  $L_2$  norm between 2 consecutive points. Subsequently, we calculate the first and second derivatives for the following:

- 1) Angle: angular velocity and angular acceleration.
- 2) Norm: velocity and acceleration.
- 3) Positions: horizontal and vertical velocity and acceleration.
- 4) Pressure: pressure variations.

These computations yield a total of 10 columns of data, which are utilized in subsequent analyses.

2) *Segmentation*: We implemented segmentation to distinguish between segments occurring on the tablet surface and those in the air. Subsequently, we computed time-independent features for the entire file, focusing either solely on points recorded on the tablet or those recorded in the air. Given that the **point task** primarily involves actions in the air, statistical computations are exclusively performed on the in-air segments. Conversely, for spiral tasks, only segments registered on the tablet are utilized. However, for writing and drawing tasks, both in-air and on-tablet segments are utilized. Notably, features based on pressure are not retained for the in-air segments, as they would be derived from a constant value.

3) *Time-Independent Features*: From the time series computed previously, we extract a range of statistics to characterize the dynamic properties of the signal, namely: the mean, the standard deviation and the amplitude of the signal.

We chose not to utilize the amplitude measure for angular velocity and acceleration, as it would always yield identical values. Furthermore, we calculated the Shannon Entropy based on the points' positions, whether on the tablet or in the air. To achieve this, we employ a Gaussian kernel density estimate (KDE) on the points'  $X$  and  $Y$  positions. This enabled us to determine the probability  $q_i$  for each point  $(x_i, y_i)$ . Shannon Entropy is then defined as  $H_s = -\sum_{i=1}^N q_i \ln(q_i)$ . Following the computation of these features, we obtained a total of 54 *task-agnostic features* across the 14 tasks.

### C. Task-Specific Features

In this section, we detail the various task-specific features we computed. We divided the presentations of the features along the four main tasks' categories proposed in Section II-B, with the addition of a section specific to the **Numbers task**.

1) *Point Tasks Features*: This section presents the features specific to the **Point Tasks**. Figure 4 depicts these features. Point Tasks are mainly used to measure the motor stability of participants and are mostly used for characterization of tremor, primarily relevant to PD or PDM (though tremor may also be observed in AD, due to copathology). Most dynamic features have already been explored as task-agnostic features, so we focused on the static features of the drawing: how symmetric and regular it is, and what the dispersion of the samples is. For this task, we calculated the geometric center of the pen's position over the digital tablet. We used this geometric center as a pivot to compare the distribution of the points with respect to the computed center, through 3 features:

- 1) **Average Radius** measures the dispersion of pen positions relative to the geometric center, providing a first measurement of stability that assesses the amplitude of variations for essential tremor.
- 2) **Standard deviation of the Radius** measures the variations in the distance from the center, a second measure more focus on dystonic tremors, for irregular vibrations.
- 3) **Average Angle** measures the average of the angle between a point and the center, which can be used as a proxy for the symmetry of the drawing. Tremor and bradykinesia in PD do not always affect all limb regions equally. An average angle  $\gg 0$  or  $\ll 0$  might implicate a strong tremor axis.

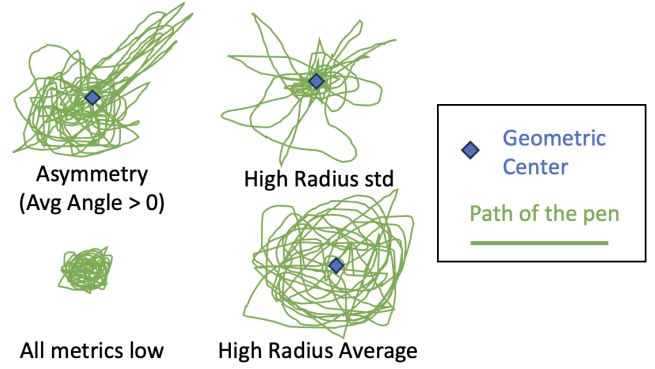


Fig. 4. Schematic of the characteristics measured by different point-tasks specific features.

2) *Spiral Tasks Features*: This section discusses static and dynamic features used to analyze hand-drawn spirals.

Those features are following three directions, illustrated in Figure 5:

- 1) Static characteristics of the ellipse bounding the spiral.
- 2) Static characteristics of the inside loops of the spiral.
- 3) Dynamic characteristics of the drawing, based on the time taken.

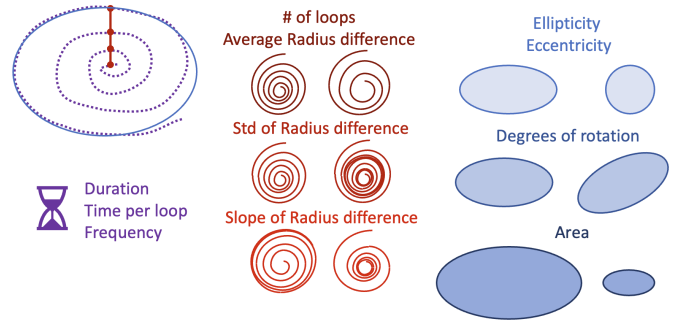


Fig. 5. Spiral-specific features computation process

a) *Ellipse characteristics*: As shown in Figure 5, the participants produce rounded spirals for all the spiral tasks. Our approach involves initially characterizing the properties of the outer boundaries of the spiral as an ellipse, leveraging these properties as features. We used Principal Component Analysis (PCA) to find the directions of the semi-major and semi-minor axes of each spiral, then find the points further away from the geometric center of the spiral in both of those directions to obtain a measure of the semi-minor axis  $a$  and the semi-major axis  $b$ . Using those values, we define a set of features:

- **Area of the ellipse**:  $Area = \pi * a * b$ .
- **Eccentricity**:  $Ec = \sqrt{1 + \frac{b^2}{a^2}}$ . The eccentricity is a scalar  $\in [0, 1[$  that measures the compression of an ellipse when defined as a conic section. An eccentricity of 0 would be the one of a circle, while an eccentricity of 1 would indicate a parabola.
- **Ellipticity**:  $El = \frac{b}{a}$ .

- **Degrees of rotation:** The angle between the semi-major axis and the abscissa.

b) *Spiral arms:* Once the outside shape has been characterized, we looked into the properties of the arms of the spiral. Each spiral is split into segments, containing each one full loop. For each loop, we computed its radius as the average distances between its points and the geometric center of the spiral, which allowed us to compute another set of features:

- **Number of loops**
- **The Average distance between loops:** the difference between 2 loops radii is defined as the distance between those 2 loops. We take the *mean* of this measure for all pairs of consecutive loops.
- **The standard deviation of the loops radius differences:** the standard deviation of the radius difference between consecutive loops. This feature quantifies the regularity of the spiral.
- **The slope of the loops radius differences:** the *slope* of the radius difference between consecutive loops.

c) *Dynamic analysis:* Dynamic features are then computed based on the total time taken to complete the task:

- **Duration:** total time taken to draw the spiral.
- **Time per loop:** the average time taken to draw one loop.
- **Frequency:** the average number of loops computed per second.

3) *Numbers Task Features:* This section focuses on the features unique to the Numbers task. Participants engaged in solving addition problems by moving down the tablet, allowing for individual analysis of each response. This methodology enabled us to track the evolution of handwriting features as participants navigate through the task. For a comprehensive breakdown of these features, please refer to Figure 6 below.

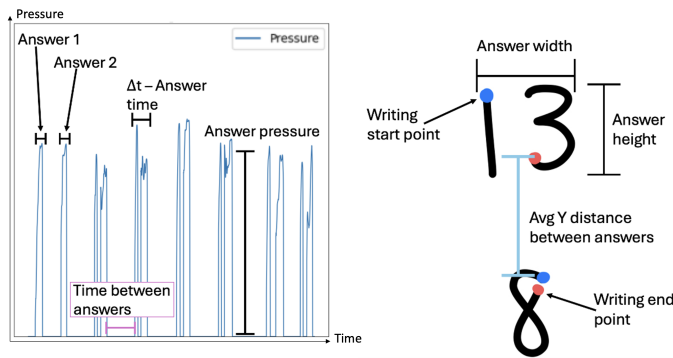


Fig. 6. Schematic of the features used for each answer of the Numbers task. The left graph shows the variations in pressures across the whole task, and the right schematic shows the features measured between 2 consecutive answers.

a) *Average Width of Answer:* The average width of each answer quantifies the size of the handwriting. It is computed by subtracting the minimum  $X$  coordinate from the maximum  $X$  coordinate for each answer and then averaging these values. People with PD have been found to have less control of their movement amplitudes and variance, resulting in compensatory longer strokes and larger handwriting under medication [49], as they are during the studied tasks.

b) *Change in Width of Answer:* The variation of width from one answer to the next. It is computed through a linear regression between the width of each answer and the question number. The feature itself represents the slope of this regression line. The variation in width is aimed to measure the presence of micrographia [43].

c) *Change in Average Answer Pressure:* The average answer pressure feature is a measure of the amount of pressure that a person applies while writing the answer. This feature can be leveraged as a time series feature to track its variation as the participant progresses through the task. It is computed through a linear regression between the average pressure of each answer and the question number. The feature itself represents the slope of this regression line. This feature might help pick up dystonia features, involuntary muscle contractions commonly seen in neurodegenerative diseases.

d) *Time per Answer:* The total duration feature measures the time a participant spends answering one of the questions. Given the absence of a predefined time limit for the Numbers task, this feature provides insight into the participant's pace in completing the task.

4) *Writing Tasks Features:* In this section, we present the features extracted from the writing tasks: **freewrite**, **copy text**, and **copy text memory** [50]. The computation of these features is shown in Figure 7.

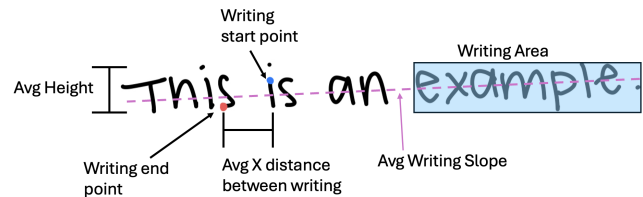


Fig. 7. Schematic of the features used in writing tasks, illustrated for the words 'This is an example'.

a) *Pressure Standard Deviation:* The pressure standard deviation feature is a measure of the spread of the amount of pressure a person applies while writing. This measures how steady the hand is when writing by capturing the variations in pressure. Only the nonzero pressure values were considered when calculating this feature, as no pressure can be computed if the pen is not touching the tablet.

b) *Average Time Between Writing:* The average time between writing measures how long it takes for the participant to start writing after finishing a word. This shows how fluent the writing is and how stable the motor planning activity is. The feature was calculated by averaging the total time the pen was not touching the tablet.

c) *Average Horizontal Distance Between Words:* This feature was calculated by finding the difference between the  $X$  value of when the pen is lifted and when it is put back down. Only the  $X$  distance was considered because the  $Y$  distance between the words is dependent on both the letters they are writing and how they write the letters.

d) *Total Time:* The total time feature gauges the duration required for task completion. It is determined by calculating the time elapsed from when the participant initially places the

pen to start writing until they lift the pen after writing the last word. This feature holds greater significance for tasks like Copy Text and Copy Read Text, where participants' required text to write is the same.

#### D. Statistical Analysis

After extracting a total of 76 features (i.e., 54 task-agnostic features and 22 task-specific features), we aim to evaluate their relevance for assessing and characterizing neurodegenerative diseases (NDs). Our objective is twofold: first, to identify which features effectively differentiate the CTL group from each of the disease groups (AD\*, PD, and PDM), and second, to assess whether handwriting features can distinguish PD from other forms of Parkinsonism (PDM).

To this end, we perform a Kruskal-Wallis H-test across the four experimental groups (CTL, AD, PD, PDM) for each feature, using the `scipy.stats.kruskal` function from the Scipy toolkit<sup>2</sup>. When a participant had multiple sessions, the average of all sessions for each feature is used, to insure the independence of all observations. For features showing a significant global effect ( $p < 0.05$ ), we apply Dunn's post hoc test to identify specific group differences. To control for false discoveries arising from multiple testing, we apply global False Discovery Rate (FDR) correction across all tasks and features for each comparison, using the `statsmodels.stats.multitest.fdr` correction function<sup>3</sup>. To complete our analysis of the separability of those groups of participants, we measured the Area Under the Curve (AUC) for pairs of participant groups, which will be presented alongside FDR-corrected p-values.

Additionally, to investigate how individual features relate to cognitive and motor functioning, we compute the Pearson correlation coefficient between each of the 76 extracted features and both the MoCA [35] (Montreal Cognitive Assessment, for all participants) and UPDRS-III [36] (Unified Parkinson's Disease Rating Scale, motor section, only measured for the PD and PDM participants) scores across participants. To provide a more detailed analysis of motor function, we also compute correlations between each feature and the individual subdomains of the UPDRS-III score, including: rigidity, upper extremity bradykinesia, lower extremity bradykinesia, arising from a chair, gait, freezing of gait, postural stability, posture, gait and posture composite, kinetic tremor, postural tremor, resting tremor, global tremor score, and non-tremor components.

Significant results from both the group comparisons and correlation analyses are presented and discussed in the following sections.

1) *Grouped features*: We hypothesized that certain features extracted for a specific type of task would exhibit consistent behavior across all tasks. To test this hypothesis, we grouped the tasks together. For each group, we conducted the same statistical comparisons outlined in section III-D. However, instead of analyzing the recordings from individual tasks, we considered all recordings within each task group. We then measured the significance of all features for each of these task groups as if they were a single task.

<sup>2</sup><https://docs.scipy.org/doc/scipy/reference/generated/scipy.stats.kruskal.html>

<sup>3</sup><https://www.statsmodels.org/dev/generated/statsmodels.stats.multitest.fdr.html>

- **All spiral tasks: Spiral dominant, Spiral non-dominant, and Spiral PaTaKa.**
- **All point tasks: Point dominant, Point non-dominant, and Point sustained.**
- **All writing tasks: Freewrite, Copy Text, and Copy Read Text.**
- **All drawing tasks: Draw Clock, Draw Cube, Copy Image, and Copy Image Memory.**

Table II summarizes the tasks at hand sorted per group and the specific features proposed per group of tasks.

TABLE II  
SUMMARY OF THE TASKS AT HAND AND THEIR SPECIFIC FEATURES.

Group	Tasks	Specific Features
Points	Point Right	Radius from centroid Angle from Centroid Std of the Radius
	Point Left	
	Point Sustained	
Spirals	Spiral Right	Area of the spiral Eccentricity Ellipticity Number of loops Distance between loops Time per loop Frequency
	Spiral Left	
	Spiral PaTaKa	
Numbers	Numbers	Avg width of answer Change in Avg pressure Time per answer
Writing	Copy Text	Pressure Ratio Pressure std. Avg time between words Avg distance between words Total time
	Copy Text Memory	
	Freewrite	
Drawing	Copy Image	CLIP similarity image-image CLIP similarity text-image
	Copy Image Memory	
	Draw Clock	
	Copy Cube	

#### E. Classification Experiments

In addition to conducting statistical analyses, we conduct binary classification experiments across various experimental groups using features extracted from each task. Namely, it involves a binary classification (e.g., AD\* vs CTL) that facilitates the assignment of samples to their corresponding groups, thereby enabling the evaluation of the features' effectiveness in distinguishing between the categories under investigation. As for the statistical analysis, the feature set used in the classification models consists of both task-specific and general features, ensuring a comprehensive representation of handwriting dynamics. The number of features varies across tasks, with Copycube, Drawclock, Copymage Memory, and Copymage containing 54 features, while Copyreadtext, Copytext, and Freewrite include 62 features. The Numbers task has 68 features, whereas Point DOM and Point NONDOM each contain 28 features, and Point Sustained has 27 features. Additionally, Spiral DOM includes 38 features, while Spiral NONDOM and Spiral Pataka each have 37 features. These features capture various aspects of handwriting, including dynamics (e.g., velocity, acceleration, jerk), spatial properties (e.g., trajectory deviations, area), and pressure dynamics (e.g., mean pressure, pressure variability).

These experiments further evaluate the discriminative power of the features and the utility of tasks in extracting valuable information for characterizing different disorders. We are employing a range of classifiers, including Random Forest (RF), Bagging (BG), and Multi-Layer Perceptron (MLP)<sup>4</sup>. For each classifier, hyperparameter tuning was performed using nested cross-validation (NCV) to ensure optimal generalization performance. Specifically, for the BG classifier, we tuned *max\_samples* (proportion of training samples used per estimator) and *n\_estimators* (number of base estimators). For the MLP classifier, we optimized *hidden\_layer\_sizes* (number of neurons in the hidden layer). Finally, for the RF classifier, we tuned *n\_estimators* (number of trees in the forest) and *max\_features* (number of features considered per split). NCV is a widely used approach for assessing model performance, especially when dealing with limited data, as it helps provide an unbiased estimate of how well the model will generalize to new data. By incorporating two levels of data partitioning, NCV enables both model evaluation and hyperparameter tuning while minimizing overfitting and overly optimistic performance estimates [51], [52]. The NCV framework consists of two levels of cross-validation to ensure robust model evaluation and mitigate overfitting. In our implementation, the *outer loop* employs a 10-fold cross-validation, partitioning the dataset into 10 folds, with one fold held out for testing while the remaining nine are used for training. Within each outer training set, an *inner 10-fold cross-validation* is conducted to optimize hyper-parameters. The best hyperparameter configuration is selected based on the *average F1-score* computed across all 10 inner folds, which helps mitigate variance in performance estimates and ensures stability in hyperparameter selection. The F1-score was chosen as the optimization criterion due to class imbalance. To prevent data leakage, cross-validation was strictly performed at the subject level. Speaker-independent folds were created to ensure that all samples from a given individual appeared only in either the training or test set within any iteration. This setup prevents data from the same subject from being in both training and testing, thereby avoiding overly optimistic performance estimates. The entire NCV process involved 100 hyperparameter tuning runs (10 outer folds  $\times$  10 inner folds), with final performance estimates derived by averaging results across the outer folds. This methodology provides a robust assessment of model generalization while maintaining strict speaker independence. For our chosen model, the Bagging Classifier, the following list of hyper-parameters was explored, and the best combination for each task was kept:

- *max\_samples*: 0.05, 0.1, 0.2, 0.5
- *n\_estimators*: 10, 100, 1000

The full list of explored hyper-parameters for every explored model is provided in the associated github<sup>5</sup>.

<sup>4</sup>To implement the different classifiers, we are using the Scikit-learn (Sklearn) library in Python. See [https://www.tutorialspoint.com/scikit\\_learn/scikit\\_learn\\_introduction.htm](https://www.tutorialspoint.com/scikit_learn/scikit_learn_introduction.htm)

<sup>5</sup>The full code allowing for the reproduction of all experiments will be released upon acceptance on github

## IV. RESULTS

In this section, we first present the most significant features obtained by groups of features for each test realized. Then, we comment on the results obtained in the classification experiments for each task.

### A. Task-agnostic Features Results

Out of 54 task-agnostic features computed, we found 53 were significant ( $p \leq 0.05$ ) for, at least one task and one groups comparison. The complete table is available in the Appendix; however, we prioritize limited sets due to the considerable number of significant features. We present the features most effectively distinguishing AD\* and PD from control participants and separate PD from PDM participants. Subsequently, we will highlight features that exhibited robust behavior across multiple comparisons.

1) *AD\* vs CTL*: Over the 54 task-agnostic features, 50 are significant ( $p \leq 0.05$ ) in comparing AD\* and CTL participants for at least one task, and 29 have p-values smaller than 0.001. We present the 10 features having the lowest p-values in Table III across all tasks. Our most significant and consistent features across all tasks are the Shannon entropy, the duration, the mean of the velocity and accelerations for point tasks, and the variations of angular velocity and acceleration for the drawing and writing tasks. We show the box plots for some of those features in Figure 9.

*Shannon entropy* is a measure of the uncertainty in a signal, showing the erratic aspect of one's handwriting, which is a marker of indecision for cognitively impaired participants. The differences measured in *linear velocity* and *linear acceleration*, as well as *duration*, all show how significantly slower AD\* participants are from the control group, presumably due to processing inefficiency. Finally, the differences in *angular velocity* and *angular acceleration* are indicators of the swiftness of the writing. For detecting AD, the most significant features were all for writing and drawing tasks, which are much more demanding cognitively than the rest of tasks and mainly consisting of tasks designed for AD\* assessment, as opposed to the point and spiral tasks.

When comparing the tasks **Copy Text** and **Copy Read Text**, the difference in velocity and horizontal acceleration is significantly higher for AD\* participants than CTL participants ( $p$ -value  $\leq 0.001$  for both), which shows how the multi-tasking has a way higher effect on cognitive participants.

A limitation of our approach here is the lower number of participant for the AD/MCI category, which did not allowed us a separated analysis of the cognitive impairments against the participants presenting only AD's signs.

2) *PD vs CTL*: Over the 54 task-agnostic features, 10 are significant ( $p \leq 0.05$ ) in the comparison between PD and CTL participants for at least one task, and 7 have p-values under 0.001. Table IV shows the top 10 features with the lowest p-values across all tasks for the PD vs. CTL comparison. These features primarily revolve around in-air dynamics, variations, and averages of velocities and angular velocities. They are notably discriminatory for point tasks. Additionally, we present box plots for these significant features in Figure 10 for further visualization and analysis.

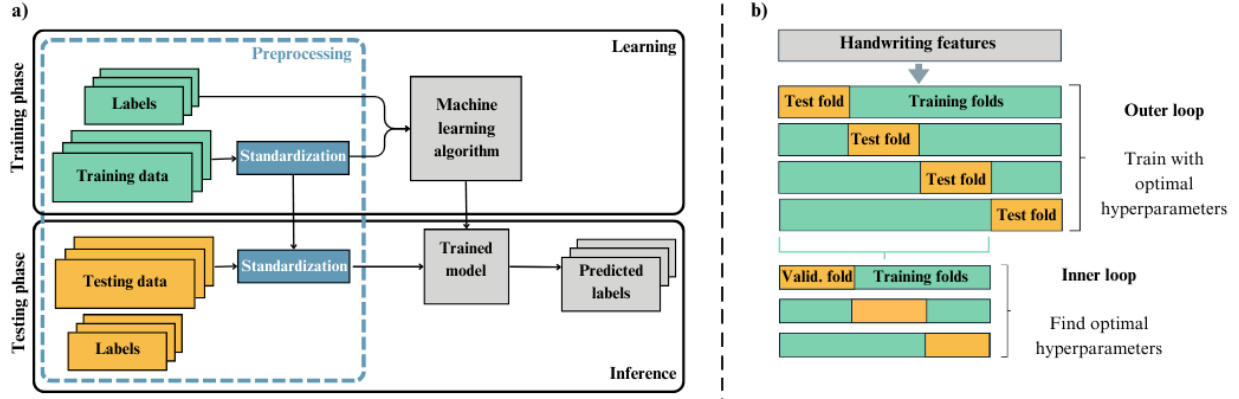


Fig. 8. a) Machine learning pipeline was adopted for training and testing. b) Nested cross-validation for algorithm selection. In the graph, the nested cross-validation process is exemplified using 3 folds for training, one for testing in the outer loop, 2 for training, and one for validating in the inner loop. However, in our experiments, we used 9 folds for training, one for testing in the outer loop, 8 for training, and one for validating in the inner loop. This strategy was applied separately when training each of the classifiers adopted in the experiments.

TABLE III

*p*-VALUES AND AUC FOR THE BEST 10 FEATURES FOR AD\* vs CTL COMPARISON. THE TABLE IS REPEATED TO FIT THE PAGE. SIGNIFICANT *p*-VALUES ARE **BOLDED**, AS WELL AS AUC VALUES OVER 0.75

AD* vs CTL	Copy Image		Copy Text		Copy Read Text	
	p-val	AUC	p-val	AUC	p-val	AUC
in-air avg. angular acc.	0.070	0.700	<b>&lt;0.001</b>	<b>0.791</b>	0.087	0.672
in-air shannon entropy	<b>&lt;0.001</b>	<b>0.873</b>	<b>&lt;0.001</b>	<b>0.887</b>	<b>&lt;0.001</b>	<b>0.827</b>
in-air std angular acc.	<b>0.019</b>	0.737	<b>&lt;0.001</b>	<b>0.818</b>	<b>0.034</b>	0.702
in-air std angular velocity	<b>0.019</b>	0.730	<b>&lt;0.001</b>	<b>0.826</b>	0.058	0.692
on-tablet avg. X acc.	<b>0.017</b>	0.732	1.000	0.605	<b>&lt;0.001</b>	<b>0.761</b>
on-tablet avg. Y acc.	0.078	0.680	1.000	0.597	<b>&lt;0.001</b>	<b>0.754</b>
AD* vs CTL	Numbers		Draw Clock		Freewrite	
	p-val	AUC	p-val	AUC	p-val	AUC
in-air avg. angular acc.	0.125	0.691	<b>&lt;0.001</b>	<b>0.761</b>	<b>&lt;0.001</b>	<b>0.760</b>
in-air shannon entropy	<b>&lt;0.001</b>	<b>0.794</b>	<b>&lt;0.001</b>	<b>0.866</b>	<b>&lt;0.001</b>	<b>0.769</b>
in-air std angular acc.	<b>0.045</b>	0.727	<b>&lt;0.001</b>	<b>0.768</b>	<b>&lt;0.001</b>	<b>0.821</b>
in-air std angular velocity	0.125	0.694	<b>&lt;0.001</b>	<b>0.799</b>	<b>&lt;0.001</b>	<b>0.774</b>
on-tablet avg. X acc.	1.000	0.535	<b>&lt;0.001</b>	<b>0.788</b>	<b>0.023</b>	0.698
on-tablet avg. Y acc.	1.000	0.597	<b>&lt;0.001</b>	<b>0.780</b>	<b>0.023</b>	0.700
AD* vs CTL	Point Dominant		Point Non Dominant		Point Sustained	
	p-val	AUC	p-val	AUC	p-val	AUC
in-air avg. angular acc.	<b>0.016</b>	0.726	1.000	0.627	<b>0.030</b>	0.740
in-air avg. acc.	<b>&lt;0.001</b>	<b>0.792</b>	<b>&lt;0.001</b>	<b>0.850</b>	<b>&lt;0.001</b>	<b>0.809</b>
in-air avg. velocity	<b>&lt;0.001</b>	<b>0.797</b>	<b>&lt;0.001</b>	<b>0.857</b>	<b>&lt;0.001</b>	<b>0.827</b>
in-air shannon entropy	<b>&lt;0.001</b>	<b>0.865</b>	<b>&lt;0.001</b>	<b>0.810</b>	<b>&lt;0.001</b>	<b>0.872</b>
in-air std angular acc.	<b>&lt;0.001</b>	<b>0.804</b>	0.117	0.708	<b>0.003</b>	<b>0.789</b>
in-air std acc.	<b>0.015</b>	0.716	<b>&lt;0.001</b>	<b>0.766</b>	0.290	0.655
in-air std velocity	0.159	0.650	<b>0.004</b>	0.737	0.390	0.647

For detecting PD, the most significant features were for drawing and point tasks. The point tasks were better suited to assess motoric features of PD, such as tremor and bradykinesia. Accordingly, we observed subjects with PD showed significantly lower *angular velocity* and *angular acceleration* in air, which could be indicators of hypometria [53]. The drawing tasks were much more complex tasks, mainly designed for cognitive evaluation but that still require basic motor skills to complete. In those tasks, the *in-air angular velocity* is still a discriminative feature, but features of variation (as standard deviation or amplitudes) of the velocity and acceleration on the tablet were notable. These findings may represent, tremor, dystonia, dyskinesia, myoclonus other other complicating motor symptoms that develop in some persons with PD [10]. However, none of the task-agnostic features measured on the spirals tasks, mainly motor tasks often used for PD assessment,

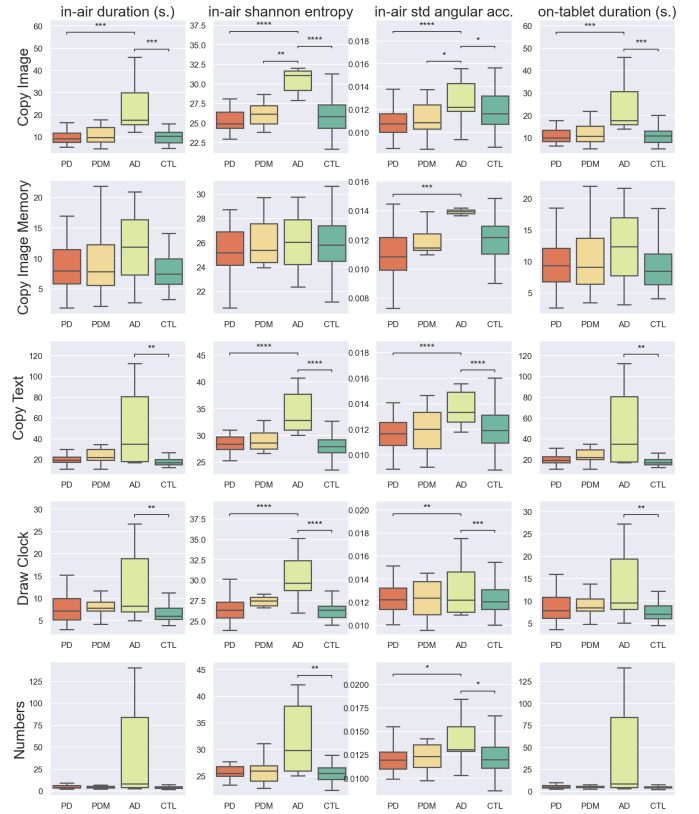


Fig. 9. Boxplots of the most significant features (AD\* vs CTL) presented across drawing and writing tasks for all groups of participants.

were discriminative enough.

3) *PD vs PDM*: Among the 54 task-agnostic features, only 6 are significant ( $p \leq 0.05$ ) in comparing PD and PDM participants for at least one task. We only found significant features for the **Spiral** tasks here.

To distinguish PD from other parkinsonism, significant variations can only be found in the **Spiral** tasks, motor exercises designed for PD assessment. We observe few significant features for the **Spiral** tasks, mostly amplitudes of *velocity* and *acceleration*, the best being for the *vertical velocity*. The

TABLE IV  
p-VALUES AND AUC FOR THE BEST 10 FEATURES FOR PD VS CTL  
COMPARISON. THE TABLE IS REPEATED TO FIT THE PAGE. SIGNIFICANT  
P-VALUES ARE **BOLDED**, AS WELL AS AUC VALUES OVER 0.75.

PD vs CTL	All Points		Point Dominant		Point Non Dominant	
	p-val	AUC	p-val	AUC	p-val	AUC
in-air avg. angular acc.	< <b>0.001</b>	0.723	<b>0.041</b>	0.723	<b>0.009</b>	<b>0.768</b>
in-air avg. acc.	<b>0.027</b>	0.611	1.000	0.611	0.443	0.624
in-air avg. X acc.	< <b>0.001</b>	0.637	0.659	0.628	<b>0.032</b>	0.694
in-air avg. Y acc.	< <b>0.001</b>	0.650	0.076	0.676	0.322	0.647
in-air avg. angular velocity	< <b>0.001</b>	0.742	<b>0.021</b>	0.743	<b>0.008</b>	<b>0.768</b>
in-air avg. velocity	<b>0.031</b>	0.608	1.000	0.620	0.437	0.630
in-air avg. X velocity	< <b>0.001</b>	0.639	1.000	0.616	0.129	0.678
in-air avg. Y velocity	< <b>0.001</b>	0.682	<b>0.041</b>	0.711	0.143	0.678
in-air std angular acc.	< <b>0.001</b>	0.723	0.052	0.738	<b>0.010</b>	<b>0.770</b>
in-air std angular velocity	< <b>0.001</b>	0.733	<b>0.021</b>	<b>0.756</b>	<b>0.009</b>	<b>0.759</b>

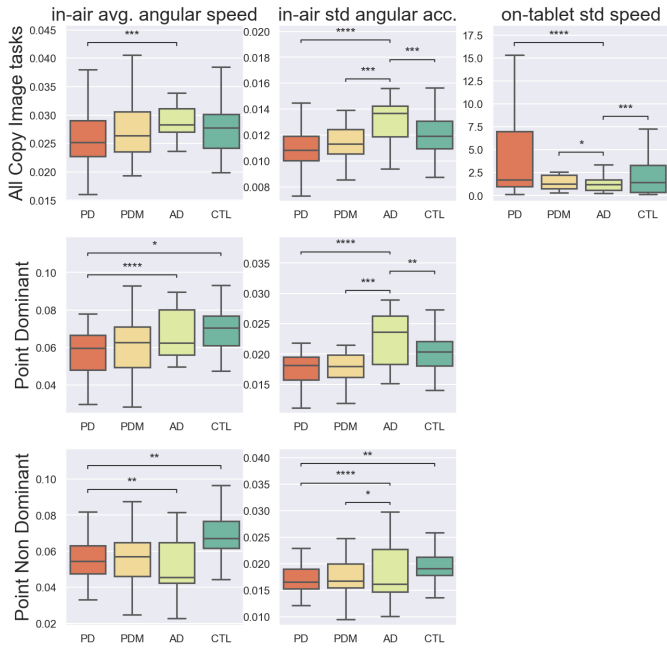


Fig. 10. Boxplots of some the best features extracted for PD vs CTL, all from angular velocity and accelerations, presented for drawing and point tasks for all groups of participants.

**Spiral** tasks reveal a difference in velocity between PD and PDM participants, the latest being slower, as shown in Figure 11.

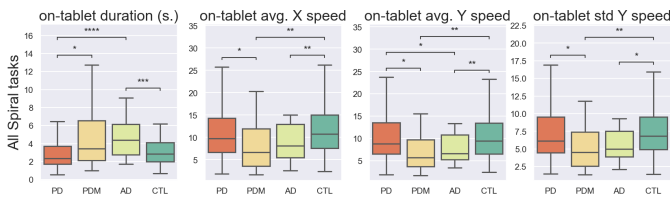


Fig. 11. Boxplots of some the best features extracted for PD vs PDM for all the spiral tasks combined.

### B. Task-Specific Results

After presenting the results of the task-agnostic features, we focus on the task-specific ones, which are crafted especially for certain tasks or groups of tasks.

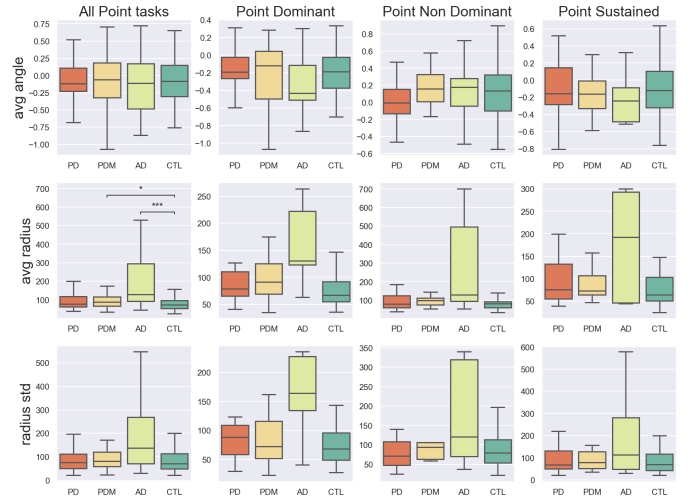


Fig. 12. Boxplots of the best point-specific features for all groups of participants.

1) *Point Tasks Results:* Figure 12 shows all features with their significance. None of the features are consistently significant across all tasks, but the *radius average* and *radius standard deviation* features exhibit the same behavior across all tasks: features from AD\* participants are higher than in the other groups. We observe a slightly higher *radius average* for PD participants compared to CTL, only significant when considering all point tasks, showing that the *Point* tasks capture only little of the expected tremors.

2) *Spiral Tasks Results:* Figure 13 shows the boxplots of the spiral-specific features that were significant for at least one of the tasks. All the features exhibit a similar behavior across all tasks: PDM and AD\* participants take more time to draw their spirals than PD and CTL, AD\* and CTL participants draw more loops, which gives a lower time per loop (*Fundamental period of the spiral*) for PDM and AD\* participants. Subjects were not instructed to provide a minimum number of loops, therefore interpretation of task duration is difficult. The reduced number of loops in the PD cohort may have been an energetically rationale choice as the task is particularly difficult with persons with impaired dexterity. As PDM represents a mixed disease cohort, few conclusions relative to PD can be drawn. It is doubtful differences are due to cognitive impairment as overall MOCA performance was similar between these groups.

3) *Numbers Task Results:* Table VI shows the Numbers-specific features' results, studying mostly the variations in time and dimensions between successive answers in the **Numbers Task**. Of the few features that show a significant difference between groups of participants, the time taken to answer is the first feature differentiating between AD\* and CTL participants, AD\* participants being slower. In a similar fashion, AD\* participants are significantly slower over time as compared to CTL participants, an effect of the increased fatigue over the various answers. Finally, we observe that both AD\* and PD participants tend to input more and more pressure over time compared to CTL participants, once again a potential fatigue indicator.

TABLE V

*p*-VALUES AND AUC OF THE SPECIFIC FEATURES FOR ALL SPIRAL TASKS SIGNIFICANT FOR AT LEAST ONE COMPARISON. SIGNIFICANT *p*-VALUES AND AUC OVER 0.75 ARE **BOLDED**.

Spirals	Feature	AD* vs CTL		CTL vs PD		PD vs PDM	
		p-val	AUC	p-val	AUC	p-val	AUC
Spirals	N loops	0.092	0.573	< <b>0.001</b>	0.604	0.303	0.538
	avg radius diff	0.141	0.557	<b>0.019</b>	0.568	0.945	0.554
	Duration	< <b>0.001</b>	0.695	0.104	0.543	<b>0.003</b>	0.623
	Number of Loops	0.370	0.563	< <b>0.001</b>	0.615	0.209	0.542
	Fundamental Period	< <b>0.001</b>	0.694	0.109	0.545	<b>0.004</b>	0.615
Dominant	Duration	< <b>0.001</b>	0.695	0.496	0.543	0.155	0.623
	Fundamental Period	< <b>0.001</b>	0.694	0.474	0.545	0.185	0.615
Non Dominant	N loops	0.714	0.573	<b>0.018</b>	0.604	0.166	0.538
	Duration	0.123	0.695	<b>0.043</b>	0.543	<b>0.028</b>	0.623
	Number of Loops	0.674	0.563	<b>0.031</b>	0.615	0.241	0.542
	Fundamental Period	0.100	0.694	0.051	0.545	<b>0.035</b>	0.615
Pataka	N loops	0.150	0.573	<b>0.012</b>	0.604	0.429	0.538
	Duration	< <b>0.001</b>	0.695	0.700	0.543	0.105	0.623
	Number of Loops	0.406	0.563	<b>0.007</b>	0.615	0.620	0.542
	Fundamental Period	< <b>0.001</b>	0.694	0.658	0.545	0.103	0.615

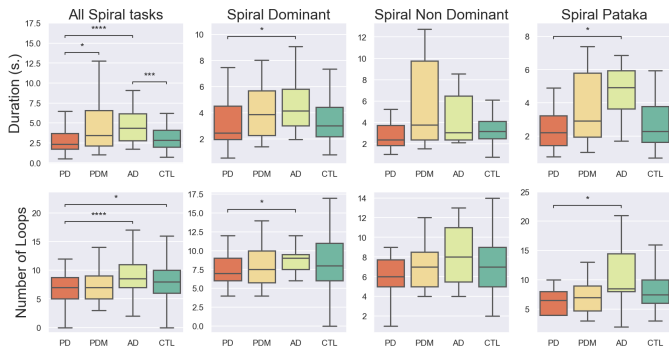


Fig. 13. Boxplots of the best spiral-specific features, for all groups of participants.

4) *Writing Tasks Results*: In this section, we present the results for the writing tasks's specific features. As shown in Figure 14, AD\* participants take a much longer *Average Time Between Writing* than all other participants across all tasks, revealing a longer hesitation and intermittent pausing times, between words. CTL participants generally have lower variations in the pressure they use than ND participants, across all tasks, a potential indicator of more stability in steadiness in the writing. PD participants use less and less pressure as they write, in contrast to the AD\* and CTL participants, and they also use a larger area to write, significant only in the **Copy Text Task**, which correlates with previous findings about PD participants writing larger than others [1].

### C. Classification Results

This subsection discusses the classification results obtained from the different handwriting tasks analyzed in this study. The results are discussed by examining each group comparison individually. The models' performance is evaluated in terms of accuracy (ACC), F-1 score (F1), and AUC. Table VIII presents results obtained using the Bagging classifier. Since the BG classifier consistently outperformed the other two classifiers we tested—RF and MLP—in terms of accuracy, F1-score, and AUROC in the different tasks considered, we present and discuss the results obtained with this classifier in the main text for the sake of simplicity. The experimental results for RF and MLP are provided in the Appendix.

TABLE VI

*p*-VALUES AND AUC OF THE SIGNIFICANT FEATURES SPECIFIC TO THE NUMBERS TASK. SIGNIFICANT *p*-VALUES AND AUC OVER 0.75 ARE **BOLDED**.

Feature	AD* vs CTL		CTL vs PD		PD vs PDM	
	p-val	AUC	p-val	AUC	p-val	AUC
time in in-air	<b>0.003</b>	0.690	0.073	0.612	0.978	0.502
avg ans time	<b>0.033</b>	0.636	0.340	0.560	0.366	0.577
change in ans width	0.203	0.581	<b>0.021</b>	0.644	0.116	0.634
change in ans pressure	<b>0.030</b>	0.639	<b>0.577</b>	0.535	0.596	0.545
change in time btwn ans	<b>0.007</b>	0.673	0.088	0.607	0.963	0.504

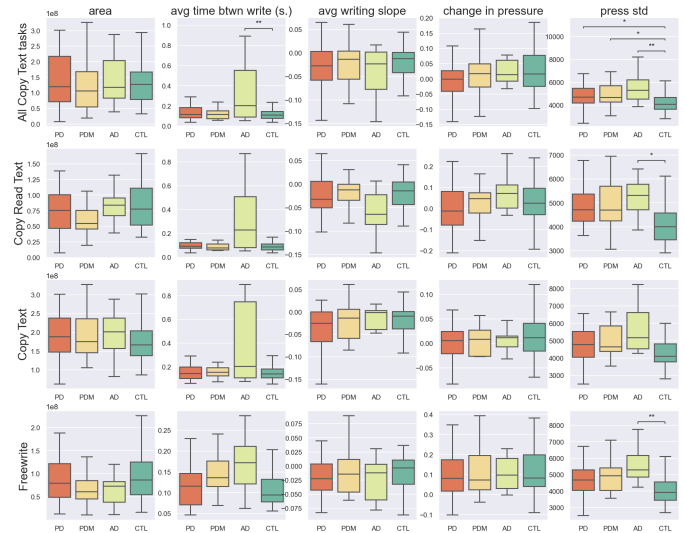


Fig. 14. Boxplots of the best writing specific features for all groups of participants.

When comparing AD\* against PD, the **Copy Image** and the **Point Dominant** tasks exhibit the best performance in terms of accuracy (91) and F1-Score (91). The **Copy Image** task involves visual perception and fine motor skills, the latter of which is particularly impaired in PD. Moreover, the **Point Non-Dominant** task reports the highest AUC score (94), indicating its efficacy in discriminating between the two conditions [54]. This is intriguing as mirror movement or mirroring dystonia have been described in Task Specific Dystonia and other movement disorders as a way to unmask and characterize latent dystonic features [55]; in our PD cohort, this task may be abnormal in PD subjects who are prone to the development of dystonic features - a finding generally thought to be absent in AD.

In the comparison between the PD and PDM group, the **Spiral PaTaKa** task stands out with the highest accuracy (73) and F1 score (71). Spiral drawing tasks are known for their sensitivity in assessing motor skills due to their complexity and demand for coordinated movements. Given the significant impact of PD on motor function, tasks like spiral drawing can provide valuable insights into motor impairment severity. The task reporting the highest AUC is **Copy Text**.

For the comparison between AD\* and CTL, the **Draw Clock** task achieves the highest accuracy (87) and F1 score (87). This task assesses the ability to draw a clock with two hands correctly placed. This complex task includes a wide

TABLE VII  
*p*-VALUES AND AUC OF THE SPECIFIC FEATURES FOR ALL SIGNIFICANT  
 WRITING TASKS. SIGNIFICANT *p*-VALUES AND AUC OVER 0.75 ARE  
**BOLDED**.

Writing	Feature	AD* vs CTL		CTL vs PD		PD vs PDM	
		<i>p</i> -val	AUC	<i>p</i> -val	AUC	<i>p</i> -val	AUC
Copy Read Text	press std	<b>0.004</b>	0.729	< <b>0.001</b>	0.700	0.602	0.542
	avg time btwn write	<b>0.012</b>	0.639	0.303	0.539	0.477	0.674
Copy Text	press std	<b>0.027</b>	0.729	<b>0.017</b>	0.700	0.508	0.542
	avg time btwn write	<b>0.004</b>	0.639	0.835	0.539	0.495	0.674
	avg x dist btwn write	<b>0.005</b>	0.617	0.459	0.507	0.967	0.647
Freewrite	press std	< <b>0.001</b>	0.729	< <b>0.001</b>	0.700	0.628	0.542
	avg time btwn write	<b>0.019</b>	0.639	0.539	0.539	<b>0.046</b>	0.674

set of skills, including adequate function of spatial awareness, executive planning, error detection, motor coordination and execution as well as language processing and numerical processing. This task is often used to screen for intra-cortical and subcortical brain network deficiencies, observed notably in individuals with early-stage dementia. The high discriminability of this task could be attributed to cognitive impairment present in the AD\* group, as indicated by their lower MoCA score compared to other groups. Additionally, the **Copy Text** and **Point Sustained** tasks yield the highest AUC, indicating their utility in distinguishing between AD\* and CTL groups.

When contrasting AD\* with PDM, the highest accuracy (83) and the F1 score (83) are achieved in the **Point Sustained** task. Given the attentional deficits commonly observed in AD, this task's effectiveness in discriminating between AD\* and CTL and PDM groups is plausible.

In comparing PD and CTL groups, the **Copy Image Memory** task displays the best performance with an accuracy and F1 score of 69. This task assesses memory function, executive function, and visuospatial skills, which are often impaired in individuals with PD compared to CTLs. Additionally, the **Copy Cube** task yields the highest AUC, indicating its effectiveness in this comparison.

Finally, when comparing the CTL and PDM groups, the **Freewrite** task emerges as the most effective, achieving the highest accuracy and F1 score of 77 and an AUC of 83. This task involves language production and cognitive flexibility, domains commonly affected in individuals with PDM compared to healthy controls. The cognitive impairment exhibited by the PDM group is further confirmed by their low MoCA score (see Table X).

#### D. Correlation of the features with UPDRS-III and MoCA scores

To further explore the clinical relevance of the extracted handwriting features, we measure the correlation between each of the 54 task-agnostic features and the MoCA score [35], which evaluates global cognitive functioning, and the motor section of the Unified Parkinson's Disease Rating Scale (UPDRS-III) [36], as well as each of the 14 subdomains of the UPDRS-III.

First we verified the normality of the distribution of the scores, and the distribution of features for each task, by using a Shapiro-Wilk test. All scores passed the normality test ( $p$ -values  $\leq 10^{-18}$ ) and all features passed the normality test ( $p$ -values  $\leq 0.037$ ).

Then we verify the linearity condition between our features and the scores previously mentioned by fitting a linear and a quadratic function to each pair of features/scores, and perform a Nested model F-test over the residual sums of squares of both functions, to find out if adding the quadratic component makes a significant difference. Most features did not pass the linearity test with the various scores (3.4% to 16.3% had a  $p$ -value under 0.05, depending on the score at hand). As most features do not pass the linearity test, we use the Spearman correlation to measure the correlation between each score and each feature.

None of the features were significantly correlated with UPDRS-III scores ( $p < 0.05$ ), suggesting limited association between our handwriting features and motor symptom severity as assessed by UPDRS-III. However, UPDRS-III is a conglomerate of many sub-domains, for which some are not related to handwriting at all. A categorical examination of each subdomain of the UPDRS-III revealed a great variation of correlations depending on the domains, as show in Table IX. The complete list of features with their individual significance is available in the appendix.

In contrast, a substantial number of features (30 out of 54) were significantly correlated with MoCA scores ( $p < 0.05$ ), indicating a strong relationship between handwriting behavior and cognitive performance. Among these, 11 features exhibited highly significant correlations with  $p$ -values below 0.0001, underscoring the potential of handwriting-based features as sensitive indicators of cognitive impairment.

## V. DISCUSSION AND CONCLUSION

The primary goal of this study was to explore the utility of handwriting as a digital biomarker for the assessment and characterization of neurodegenerative diseases (NDs), including Alzheimer's disease (AD), Parkinson's disease (PD), and related Parkinsonian disorders (PDM). We introduced a novel dataset collected at Johns Hopkins Hospital from 113 participants (46 healthy controls and 73 ND patients) who completed 14 structured handwriting tasks on a digital tablet. This rich dataset comprises 1840 handwriting recordings and is part of a broader multimodal acquisition effort that also includes synchronized speech and eye-tracking data.

We proposed and evaluated a large array of interpretable handwriting features designed to capture motor, cognitive, and behavioral markers from handwriting signals. These features were categorized as either task-agnostic (general signal descriptors applicable across tasks) or task-specific (features tailored to the expected behavior in particular task types). Our aim was to assess the ability of these features to distinguish between ND subtypes and healthy controls using statistical analysis and binary classification experiments, while ensuring clinical interpretability and relevance.

#### A. Task-Agnostic and Task-Specific Features: Findings and Limitations

Our analysis of task-agnostic features, those computed independently of the specific task performed, demonstrated that a substantial number (53 out of 54) significantly differentiated at least one group comparison (e.g., PD vs. control, AD\* vs. PDM). These features included velocity, acceleration, angular

TABLE VIII

CLASSIFICATION RESULTS FOR PAIRWISE GROUP COMPARISONS, USING THE BAGGING MODEL. THE TABLE REPORTS EXPERIMENTAL RESULTS IN TERMS OF ACCURACY (ACC), F1-SCORE (F1), AND AUC FOR EACH COMPARISON. THE BEST RESULTS FOR EACH FEATURE FOR EACH GROUP COMPARISON ARE INDICATED IN BOLD, WHILE THE SECOND-BEST ARE ITALICIZED.

Task	AD* vs PD			PD vs PDM			AD* vs CTL			AD* vs PDM			PD vs CTL			PDM vs CTL		
	ACC	F1	AUC	ACC	F1	AUC	ACC	F1	AUC	ACC	F1	AUC	ACC	F1	AUC	ACC	F1	AUC
Copy Cube	71	68	81	50	48	57	67	66	69	67	64	69	64	63	<b>71</b>	57	51	55
Draw Clock	86	86	90	56	55	61	<b>87</b>	<b>87</b>	88	79	77	71	60	60	54	67	53	39
Copy Image	<b>91</b>	<b>91</b>	91	67	53	46	82	82	86	78	77	<i>81</i>	48	48	54	56	52	35
Copy Image Memory	73	73	83	65	51	51	64	63	62	67	67	63	<b>69</b>	<b>69</b>	69	54	48	47
Copy Read Text	77	75	81	59	44	35	67	67	72	76	74	78	61	60	62	71	69	79
Copy Text	77	78	88	63	58	<b>74</b>	81	82	<b>89</b>	73	72	<b>83</b>	63	63	64	67	65	66
Freewrite	69	69	76	66	52	45	71	71	75	73	70	65	48	48	47	<b>77</b>	<b>77</b>	<b>83</b>
Numbers	69	69	72	57	49	45	68	68	75	63	57	53	55	55	53	65	51	42
Point Dominant	<b>91</b>	<b>91</b>	93	66	52	47	84	84	85	82	82	78	66	65	68	57	55	53
Point Non-Dominant	84	84	<b>94</b>	67	56	52	85	84	85	73	71	72	68	68	66	71	71	72
Point Sustained	89	89	92	67	54	59	80	80	<b>89</b>	<b>83</b>	<b>83</b>	79	62	62	69	65	65	59
Spiral Dominant	67	64	69	67	53	50	60	60	63	75	69	57	54	52	54	60	57	60
Spiral Non-Dominant	65	63	59	64	63	66	57	55	58	79	78	64	41	41	33	60	57	50
Spiral PaTaKa	70	68	71	<b>73</b>	<b>71</b>	51	64	61	56	73	68	68	60	60	61	<b>77</b>	76	69

TABLE IX

NUMBER OF FEATURES OVER THE 54 TASK-AGNOSTIC FEATURES PRODUCED BEING CORRELATED WITH MoCa SCORE, UPDRS-III SCORE AND ITS SUB-COMPONENTS.

Score	$p\_value <$			
	0.05	0.01	$10^{-3}$	$10^{-4}$
MoCa [35]	30	18	11	9
UPDRS-III [36]	0	0	0	0
Rigidity	0	0	0	0
Upper bradykinesia	2	2	0	0
Lower bradykinesia	28	17	2	0
Arising from chair	15	4	1	0
Gait	19	0	0	0
Freeze of gait	16	6	0	0
Postural stability	7	3	0	0
Posture	0	0	0	0
Gait and posture composite	0	0	0	0
Kinetic tremor	22	0	0	0
Postural Tremor	6	2	0	0
Resting tremor	6	0	0	0
Global tremor	33	3	0	0
Non-tremor components	1	0	0	0

velocity, entropy, and timing-related features. Notably, these general features were consistent across task categories and aligned with known ND symptomatology. For example, reduced velocity and increased entropy were particularly salient in AD\* participants, aligning with executive dysfunction and impaired motor planning.

However, the task-agnostic approach also revealed limitations. While general features captured high-level differences, they occasionally failed to detect hallmark disease-specific signs. Most notably, micrographia, a classic symptom of PD, was not captured in a statistically significant way. This suggests that some ND-specific features may only manifest under conditions that tightly control for task type, hand dominance, or cognitive load.

To address this limitation, we introduced task-specific features, tailored to the intent and structure of each task. These revealed more nuanced and disease-relevant patterns. AD\* participants showed longer in-air times, slower execution, and greater pressure variability, particularly during cognitively demanding tasks such as paragraph writing and arithmetic. PD participants drew fewer spiral loops, moved more slowly during motor tasks, and exhibited greater pressure variability, overlapping with patterns observed in the PDM group. While the PDM group was younger, its behavior often fell between the PD and control groups, suggesting that our features are relatively robust to age differences.

Despite these strengths, cross-task comparisons (such as between dominant and non-dominant hand usage or between reading and non-reading conditions) showed limited discriminative power, with the exception of Copy Text versus Copy Read Text. These results suggest the need for more advanced methods to capture inter-task behavioral adaptations.

#### B. Classification Performance and Observed Limitations

In this study, we prioritized classification using interpretable features, incorporating task-specific and general features across handwriting tasks. Our primary goal was to develop a model that provides meaningful insights into the motor and cognitive impairments associated with neurodegenerative diseases, ensuring that the extracted features remain clinically interpretable. This approach allows for a better understanding of the underlying mechanisms driving classification decisions, which is crucial for real-world applications in clinical settings. However, deep learning-based approaches, such as those leveraging raw handwriting images or spectrogram representations of handwriting signals, offer a promising alternative. In a recent study [56], we explored non-interpretable methods by applying CNN and CNN-BLSTM models to spectrogram representations of handwriting signals for neurodegenerative disease classification. Our results demonstrated that classification performance varied across handwriting tasks and spectrogram channel combinations, with CNN consistently

outperforming CNN-BLSTM. While the current study focused on interpretable features, future work could investigate hybrid approaches integrating deep learning techniques with interpretable models to enhance classification performance while maintaining clinical transparency. This would allow for the benefits of deep learning's feature extraction capabilities while ensuring that the results remain interpretable and useful for clinical decision-making.

### C. Clinical Applications and Implications

Handwriting analysis has strong potential as a non-invasive, low-cost, and accessible digital biomarker. It captures both motor and cognitive processes and can be easily deployed using commercial tablets or styluses. Clinically, such tools could support early screening, aid differential diagnosis, and monitor disease progression or response to treatment. The features developed in this study are interpretable and aligned with known clinical features, making them suitable for real-world use.

While handwriting analysis shows significant promise as a digital biomarker for neurodegenerative diseases, the current equipment setup remains a notable limitation for widespread clinical adoption. The data in this study were collected using a high-resolution graphics tablet capable of capturing position, pressure, and in-air movements with high precision. However, this hardware is relatively expensive and requires controlled conditions and trained personnel for operation. These factors restrict its applicability outside research environments and limit deployment in routine clinical settings or home-based assessments.

### D. Discussion

While the proposed features and classification results offer compelling evidence for the utility of handwriting in distinguishing neurodegenerative conditions, there are several limitations that affect generalizability. First, the models developed in this study are trained on a dataset collected under tightly controlled conditions with a homogeneous set of equipment and task protocols. Their applicability to new populations, clinical settings, or hardware setups remains to be validated. This lack of generalization could be addressed through the use of pre-trained systems, such as neural networks which can learn more transferable representations, or through the use of more diverse handwriting datasets.

Additionally, while handwriting captures a rich combination of motor and cognitive activity, it is only one window into neurodegeneration. The broader dataset collected in this study also includes speech and eye-tracking data, which have yet to be analyzed in combination with handwriting. Multimodal approaches are likely to improve both sensitivity and specificity by modeling interactions across domains such as language, motor planning, and attention.

Finally, extending the current dataset by increasing the number of participants, balancing demographic variables, and adding more task repetitions will improve statistical power and enable more reliable model development and evaluation.

### E. General Conclusion and Future Directions

This study introduced a diverse set of interpretable features for handwriting analysis and demonstrated their value

in differentiating between neurodegenerative conditions using data from structured tablet-based tasks. The results validate handwriting as a meaningful digital biomarker and provide a strong foundation for future research and clinical translation.

Building on this work, our future efforts will focus on four main directions. First, we plan to increase the size and diversity of our dataset to improve model robustness and enable the study of more subtle effects, such as early-stage impairments and cross-condition overlap. Second, we will integrate the available speech and eye-tracking data to explore multimodal models that can capture interaction effects across cognitive and motor channels. Third, we will investigate neural network-based solutions, including the use of pre-trained models, to leverage broader datasets and improve generalizability across populations and devices. Finally, we will evaluate the performance of our models on more portable and affordable equipment, with the goal of developing lightweight and scalable tools suitable for deployment in real-world clinical and home settings.

Together, these future directions aim to bridge the gap between research prototypes and practical, interpretable, and accessible tools for early detection and monitoring of neurodegenerative diseases.

## REFERENCES

- [1] M. Thomas, A. Lenka, and P. Kumar Pal, "Handwriting analysis in parkinson's disease: current status and future directions," *Movement disorders clinical practice*, vol. 4, no. 6, pp. 806–818, 2017.
- [2] T. Thebaud, C. Chen, L. Moro-Velazquez, N. Dehak, and E. S. Oh, "Handwriting characteristics analysis for alzheimer's disease and mild cognitive impairments assessment," *Alzheimer's & Dementia*, vol. 19, p. e082245, 2023.
- [3] P. Werner, S. Rosenblum, G. Bar-On, J. Heinik, and A. Korczyn, "Handwriting process variables discriminating mild alzheimer's disease and mild cognitive impairment," *The Journals of Gerontology Series B: Psychological Sciences and Social Sciences*, vol. 61, no. 4, pp. P228–P236, 2006.
- [4] A. Ünlü, R. Brause, and K. Krakow, "Handwriting analysis for diagnosis and prognosis of parkinson's disease," in *Biological and Medical Data Analysis: 7th International Symposium, ISBMDA 2006, Thessaloniki, Greece, December 7-8, 2006. Proceedings 7*. Springer, 2006, pp. 441–450.
- [5] S. Rosenblum, M. Samuel, S. Zlotnik, I. Erikh, and I. Schlesinger, "Handwriting as an objective tool for parkinson's disease diagnosis," *Journal of neurology*, vol. 260, pp. 2357–2361, 2013.
- [6] P. Drotár, J. Mekyska, I. Rektorová, L. Masarová, Z. Smékal, and M. Faundez-Zanuy, "Evaluation of handwriting kinematics and pressure for differential diagnosis of parkinson's disease," *Artificial intelligence in Medicine*, vol. 67, pp. 39–46, 2016.
- [7] —, "Decision support framework for parkinson's disease based on novel handwriting markers," *IEEE Transactions on Neural Systems and Rehabilitation Engineering*, vol. 23, no. 3, pp. 508–516, 2014.
- [8] —, "Analysis of in-air movement in handwriting: A novel marker for parkinson's disease," *Computer methods and programs in biomedicine*, vol. 117, no. 3, pp. 405–411, 2014.
- [9] J. Mucha, J. Mekyska, Z. Galaz, M. Faundez-Zanuy, K. Lopez-de Ipina, V. Zvoncak, T. Kiska, Z. Smekal, L. Brabenec, and I. Rektorova, "Identification and monitoring of parkinson's disease dysgraphia based on fractional-order derivatives of online handwriting," *Applied Sciences*, vol. 8, no. 12, p. 2566, 2018.
- [10] E. J. Smits, A. J. Tolonen, L. Cluitmans, M. Van Gils, B. A. Conway, R. C. Zietsma, K. L. Leenders, and N. M. Maurits, "Standardized handwriting to assess bradykinesia, micrographia and tremor in parkinson's disease," *PLoS one*, vol. 9, no. 5, p. e97614, 2014.
- [11] C. P. Fernandes, G. Montalvo, M. Caligiuri, M. Pertsinakis, and J. Guimaraes, "Handwriting changes in alzheimer's disease: A systematic review," *Journal of Alzheimer's Disease*, vol. 96, no. 1, pp. 1–11, 2023.

- [12] N. D. Cilia, G. De Gregorio, C. De Stefano, F. Fontanella, A. Marcelli, and A. Parziale, "Diagnosing alzheimer's disease from on-line handwriting: A novel dataset and performance benchmarking," *Engineering Applications of Artificial Intelligence*, vol. 111, p. 104822, 2022.
- [13] J. Garre-Olmo, M. Faúndez-Zanuy, K. López-de Ipiña, L. Calvó-Pexas, and O. Turró-Garriga, "Kinematic and pressure features of handwriting and drawing: preliminary results between patients with mild cognitive impairment, alzheimer disease and healthy controls," *Current Alzheimer Research*, vol. 14, no. 9, pp. 960–968, 2017.
- [14] G. Pirlo, M. Diaz, M. A. Ferrer, D. Impedovo, F. Occhionero, and U. Zurlo, "Early diagnosis of neurodegenerative diseases by handwritten signature analysis," in *International Conference on Image Analysis and Processing*. Springer, 2015, pp. 290–297.
- [15] C. R. Pereira, D. R. Pereira, F. A. Da Silva, C. Hook, S. A. Weber, L. A. Pereira, and J. P. Papa, "A step towards the automated diagnosis of parkinson's disease: Analyzing handwriting movements," in *2015 IEEE 28th international symposium on computer-based medical systems*. Ieee, 2015, pp. 171–176.
- [16] C. R. Pereira, S. A. Weber, C. Hook, G. H. Rosa, and J. P. Papa, "Deep learning-aided parkinson's disease diagnosis from handwritten dynamics," in *2016 29th SIBGRAP conference on graphics, patterns and images (SIBGRAP)*. Ieee, 2016, pp. 340–346.
- [17] P. Zham, D. K. Kumar, P. Dabnichki, S. Poosapadi Arjunan, and S. Raghav, "Distinguishing different stages of parkinson's disease using composite index of speed and pen-pressure of sketching a spiral," *Frontiers in neurology*, vol. 8, p. 268142, 2017.
- [18] K. Sarin, M. Bardamova, M. Svetlakov, N. Koryshev, R. Ostapenko, A. Hodashinskaya, and I. Hodashinsky, "A three-stage fuzzy classifier method for parkinson's disease diagnosis using dynamic handwriting analysis," *Decision Analytics Journal*, vol. 8, p. 100274, 2023.
- [19] D. Impedovo and G. Pirlo, "Dynamic handwriting analysis for the assessment of neurodegenerative diseases: a pattern recognition perspective," *IEEE reviews in biomedical engineering*, vol. 12, pp. 209–220, 2018.
- [20] V. Miler Jerkovic, V. Kojic, N. Dragasevic Miskovic, T. Djukic, V. S. Kostic, and M. B. Popovic, "Analysis of on-surface and in-air movement in handwriting of subjects with parkinson's disease and atypical parkinsonism," *Biomedical Engineering/Biomedizinische Technik*, vol. 64, no. 2, pp. 187–194, 2019.
- [21] C. Allone, V. Lo Buono, F. Corallo, L. Bonanno, R. Palmeri, G. Di Lorenzo, A. Marra, P. Bramanti, and S. Marino, "Cognitive impairment in parkinson's disease, alzheimer's dementia, and vascular dementia: the role of the clock-drawing test," *Psychogeriatrics*, vol. 18, no. 2, pp. 123–131, 2018.
- [22] M. F. De Pandis, M. Galli, S. Vimercati, V. Cimolin, M. V. De Angelis, and G. Albertini, "A new approach for the quantitative evaluation of the clock drawing test: Preliminary results on subjects with parkinson's disease," *Neurology research international*, vol. 2010, no. 1, p. 283890, 2010.
- [23] N. D. Cilia, C. De Stefano, F. Fontanella, M. Molinara, and A. Scotto Di Freca, "Using handwriting features to characterize cognitive impairment," in *Image Analysis and Processing—ICIAP 2019: 20th International Conference, Trento, Italy, September 9–13, 2019, Proceedings, Part II 20*. Springer, 2019, pp. 683–693.
- [24] A. Favaro, N. Dehak, T. Thebaud, J. Villalba, E. Oh, and L. Moro-Velázquez, "Discovering Invariant Patterns of Cognitive Decline Via an Automated Analysis of the Cookie Thief Picture Description Task," in *Proc. The Speaker and Language Recognition Workshop (Odyssey 2024)*, 2024, pp. 201–208.
- [25] A. Favaro, T. Thebaud, N. Dehak, A. Butala, E. S. Oh, and L. Moro-Velázquez, "Analyzing attention focus in the cookie theft picture description task using word alignment," in *Alzheimer's Association International Conference*. ALZ, 2024.
- [26] A. Favaro, N. Dehak, T. Thebaud, E. S. Oh, and L. Moro-Velázquez, "Evaluation of interpretable speech biomarkers for monitoring alzheimer's disease and mild cognitive impairment progression," *Alzheimer's & Dementia*, vol. 19, p. e080449, 2023.
- [27] A. Favaro, Y.-T. Tsai, A. Butala, T. Thebaud, J. Villalba, N. Dehak, and L. Moro-Velázquez, "Interpretable speech features vs. dnn embeddings: What to use in the automatic assessment of parkinson's disease in multilingual scenarios," *Computers in Biology and Medicine*, vol. 166, p. 107559, 2023.
- [28] A. Favaro, C. Motley, T. Cao, M. Iglesias, A. Butala, E. S. Oh, R. D. Stevens, J. Villalba, N. Dehak, and L. Moro-Velázquez, "A multi-modal array of interpretable features to evaluate language and speech patterns in different neurological disorders," in *2022 IEEE Spoken Language Technology Workshop (SLT)*. IEEE, 2023, pp. 532–539.
- [29] A. Favaro, L. Moro-Velázquez, A. Butala, C. Motley, T. Cao, R. D. Stevens, J. Villalba, and N. Dehak, "Multilingual evaluation of interpretable biomarkers to represent language and speech patterns in parkinson's disease," *Frontiers in Neurology*, vol. 14, p. 1142642, 2023.
- [30] Y. Wang, A. Favaro, T. Thebaud, J. Villalba, N. Dehak, and L. Moro-Velázquez, "Exploring the complementary nature of speech and eye movements for profiling neurological disorders," *Interspeech Proceedings*, 2024.
- [31] G. M. McKhann, D. S. Knopman, H. Chertkow, B. T. Hyman, C. R. Jack Jr, C. H. Kawas, W. E. Klunk, W. J. Koroshetz, J. J. Manly, R. Mayeux *et al.*, "The diagnosis of dementia due to alzheimer's disease: Recommendations from the national institute on aging-alzheimer's association workgroups on diagnostic guidelines for alzheimer's disease," *Alzheimer's & dementia*, vol. 7, no. 3, pp. 263–269, 2011.
- [32] A. Bieger, W. S. Brum, W. V. Borelli, J. Theriault, M. A. De Bastiani, A. G. Moreira, A. L. Benedet, J. P. Ferrari-Souza, J. C. Da Costa, D. O. Souza *et al.*, "Influence of different diagnostic criteria on alzheimer disease clinical research," *Neurology*, vol. 103, no. 5, p. e209753, 2024.
- [33] M. S. Albert, S. T. DeKosky, D. Dickson, B. Dubois, H. H. Feldman, N. C. Fox, A. Gamst, D. M. Holtzman, W. J. Jagust, R. C. Petersen *et al.*, "The diagnosis of mild cognitive impairment due to alzheimer's disease: recommendations from the national institute on aging-alzheimer's association workgroups on diagnostic guidelines for alzheimer's disease," *Focus*, vol. 11, no. 1, pp. 96–106, 2013.
- [34] R. B. Postuma, D. Berg, M. Stern, W. Poewe, C. W. Olanow, W. Oertel, J. Obeso, K. Marek, I. Litvan, A. E. Lang *et al.*, "Mds clinical diagnostic criteria for parkinson's disease," *Movement disorders*, vol. 30, no. 12, pp. 1591–1601, 2015.
- [35] P. Julayanont and Z. S. Nasreddine, "Montreal cognitive assessment (moca): concept and clinical review," *Cognitive screening instruments: A practical approach*, pp. 139–195, 2017.
- [36] M. D. S. T. F. on Rating Scales for Parkinson's Disease, "The unified parkinson's disease rating scale (updrs): status and recommendations," *Movement Disorders*, vol. 18, no. 7, pp. 738–750, 2003.
- [37] R. J. Elble and A. Ellenbogen, "Digitizing tablet and fahn–tolosa–marín ratings of archimedes spirals have comparable minimum detectable change in essential tremor," *Tremor and Other Hyperkinetic Movements*, vol. 7, 2017.
- [38] A. B. Hernandez, D. S. Berry, N. Grill, T. M. Hall, A. Burkes, A. Ghanem, V. D. Sharma, and E. D. Louis, "Whiget and tetras ratings of action tremor in patients with essential tremor: Substantial association and agreement," *Tremor and Other Hyperkinetic Movements*, vol. 14, 2024.
- [39] C. R. Pereira, D. R. Pereira, G. H. Rosa, V. H. Albuquerque, S. A. Weber, C. Hook, and J. P. Papa, "Handwritten dynamics assessment through convolutional neural networks: An application to parkinson's disease identification," *Artificial intelligence in medicine*, vol. 87, pp. 67–77, 2018.
- [40] R. Saunders-Pullman, C. Derby, K. Stanley, A. Floyd, S. Bressman, R. B. Lipton, A. Deligtisch, L. Severt, Q. Yu, M. Kurtis *et al.*, "Validity of spiral analysis in early parkinson's disease," *Movement disorders: official journal of the Movement Disorder Society*, vol. 23, no. 4, pp. 531–537, 2008.
- [41] K. Stanley, J. Hagenah, N. Brüggemann, K. Reetz, L. Severt, C. Klein, Q. Yu, C. Derby, S. Pullman, and R. Saunders-Pullman, "Digitized spiral analysis is a promising early motor marker for parkinson disease," *Parkinsonism & related disorders*, vol. 16, no. 3, pp. 233–234, 2010.
- [42] D. Carfora, S. Kim, N. Houmani, S. Garcia-Salicetti, and A.-S. Rigaud, "On extracting digitized spiral dynamics' representations: A study on transfer learning for early alzheimer's detection," *Bioengineering*, vol. 9, no. 8, p. 375, 2022.
- [43] J. McLennan, K. Nakano, H. Tyler, and R. Schwab, "Micrographia in parkinson's disease," *Journal of the neurological sciences*, vol. 15, no. 2, pp. 141–152, 1972.
- [44] A. Letanneux, J. Danna, J.-L. Velay, F. Viallet, and S. Pinto, "From micrographia to parkinson's disease dysgraphia," *Movement Disorders*, vol. 29, no. 12, pp. 1467–1475, 2014.
- [45] X. Zhang, L. Lv, G. Min, Q. Wang, Y. Zhao, and Y. Li, "Overview of the complex figure test and its clinical application in neuropsychiatric disorders, including copying and recall," *Frontiers in neurology*, vol. 12, p. 680474, 2021.
- [46] M. Freedman, *Clock drawing: A neuropsychological analysis*. Oxford University Press, 1994.
- [47] D. A. Cahn-Weiner, K. Williams, J. Grace, G. Tremont, H. Westervelt, and R. A. Stern, "Discrimination of dementia with lewy bodies from alzheimer disease and parkinson disease using the clock drawing test," *Cognitive and behavioral neurology*, vol. 16, no. 2, pp. 85–92, 2003.

- [48] X.-Y. Bu, X.-G. Luo, C. Gao, Y. Feng, H.-M. Yu, Y. Ren, H. Shang, and Z.-Y. He, "Usefulness of cube copying in evaluating clinical profiles of patients with parkinson disease," *Cognitive and Behavioral Neurology*, vol. 26, no. 3, pp. 140–145, 2013.
- [49] A. Van Gemmert, H.-L. Teulings, J. L. Contreras-Vidal, and G. Stelmach, "Parkinsons disease and the control of size and speed in handwriting," *Neuropsychologia*, vol. 37, no. 6, pp. 685–694, 1999.
- [50] C. Chen, T. Thebaud, A. Butala, N. Dehak, L. Moro-Velazquez, and E. S. Oh, "Cognitive assessment through writing tasks," in *Alzheimer's Association International Conference*. ALZ, 2024.
- [51] G. C. Cawley and N. L. Talbot, "On over-fitting in model selection and subsequent selection bias in performance evaluation," *The Journal of Machine Learning Research*, vol. 11, pp. 2079–2107, 2010.
- [52] I. Tsamardinis, A. Rakhshani, and V. Lagani, "Performance-estimation properties of cross-validation-based protocols with simultaneous hyperparameter optimization," *International Journal on Artificial Intelligence Tools*, vol. 24, no. 05, p. 1540023, 2015.
- [53] M. P. Broderick, A. W. Van Gemmert, H. A. Shill, and G. E. Stelmach, "Hypometria and bradykinesia during drawing movements in individuals with parkinson's disease," *Experimental brain research*, vol. 197, pp. 223–233, 2009.
- [54] G. José Luvizutto, T. Souza Silva Brito, E. de Moura Neto, and L. Aparecida Pascucci Sande de Souza, "Altered visual and proprioceptive spatial perception in individuals with parkinson's disease," *Perceptual and motor skills*, vol. 127, no. 1, pp. 98–112, 2020.
- [55] A. Quattrone, A. Latorre, F. Magrinelli, E. Mulroy, R. Rajan, R. J. Neo, A. Quattrone, J. C. Rothwell, and K. P. Bhatia, "A reflection on motor overflow, mirror phenomena, synkinesia and entrainment," *Movement Disorders Clinical Practice*, vol. 10, no. 9, pp. 1243–1252, 2023.
- [56] S. Laouedj, Y. Wang, J. Villalba, T. Thebaud, L. Moro-Velazquez, and N. Dehak, "Detecting neurodegenerative diseases using frame-level handwriting embeddings," *arXiv preprint arXiv:2502.07025*, 2025.

## APPENDIX

TABLE X  
NUMBER OF FILES AND PARTICIPANTS FOR EACH TASK AND EACH EXPERIMENTAL GROUP. THE SYMBOL  $\Sigma$  DENOTES THE TOTAL COUNT ACROSS EXPERIMENTAL GROUPS FOR A GIVEN TASK.

Task (Code)	# Files					# Participants				
	CTL	PD	PDM	AD	$\Sigma$	CTL	PD	PDM	AD	$\Sigma$
Copy Cube (CC)	38	25	14	39	116	36	22	12	20	90
Copy Image (CI)	42	37	16	42	137	39	34	14	21	108
Copy Image Memory (CM)	41	33	15	21	110	38	30	13	13	94
Copy Read Text (CR)	42	28	16	42	128	39	25	13	21	98
Copy Text (CT)	42	34	15	44	135	39	31	13	20	103
Draw Clock (DC)	43	27	15	41	126	40	24	13	20	97
Freewrite (F)	43	35	16	46	140	41	32	14	21	108
Numbers (N)	45	35	17	34	131	41	33	15	19	108
Point Dominant (PD)	44	36	16	43	139	41	32	13	21	107
Point Non-Dominant (PN)	43	36	17	43	139	40	33	14	21	108
Point Left (PL)	44	36	17	43	140	41	33	14	21	109
Point Right (PR)	43	36	16	43	138	40	32	13	21	106
Point Sustained (PS)	40	34	15	40	129	38	31	13	21	103
Spiral Dominant (SD)	41	36	16	45	138	38	33	14	21	106
Spiral Non-Dominant (SN)	41	36	15	45	137	40	33	13	21	107
Spiral Left (SL)	43	36	16	45	140	40	33	14	21	108
Spiral Right (SR)	39	36	15	45	135	38	33	13	21	105
Spiral Pataka (SP)	43	32	16	44	135	40	29	14	20	103
Total	588	464	219	569	1840	42	35	15	21	113

TABLE XI

CORRELATION OF ALL THE TASK-AGNOSTIC METRICS WITH THE MoCa SCORE, UPDRS-III SCORE AND ALL ITS SUB-COMPONENTS. 'N.S.' IS USED FOR NON SIGNIFICANT FEATURES, \* FOR P-VALUES < 0.05, \*\* FOR P-VALUES < 0.01, \*\*\* FOR P-VALUES < 0.001, AND \*\*\*\* FOR P-VALUES < 0.0001.

Feature name	MoCa [35]	UPDRS-III [36]	Rigidity	Upper bradykinesia	Lower bradykinesia	Arising from chair	Gait	Freeze of gait	Postural stability	Posture	Gait and posture composite	Kinetic tremor	Postural tremor	Resting tremor	Global tremor	Non-tremor components
in-air duration	****	n.s.	n.s.	n.s.	n.s.	n.s.	*	n.s.	n.s.	n.s.	n.s.	n.s.	n.s.	n.s.	**	n.s.
in-air avg. X speed	*	n.s.	n.s.	n.s.	n.s.	n.s.	n.s.	n.s.	n.s.	n.s.	n.s.	*	**	n.s.	*	n.s.
in-air std X speed	*	n.s.	n.s.	n.s.	n.s.	n.s.	n.s.	n.s.	n.s.	n.s.	n.s.	n.s.	*	n.s.	*	n.s.
in-air amp X speed	n.s.	n.s.	n.s.	n.s.	n.s.	n.s.	n.s.	*	n.s.	n.s.	n.s.	n.s.	n.s.	n.s.	n.s.	n.s.
in-air avg. X acc.	*	n.s.	n.s.	n.s.	n.s.	n.s.	n.s.	n.s.	n.s.	n.s.	n.s.	n.s.	*	n.s.	*	n.s.
in-air std X acc.	*	n.s.	n.s.	n.s.	n.s.	n.s.	n.s.	n.s.	n.s.	n.s.	n.s.	n.s.	n.s.	n.s.	*	n.s.
in-air amp X acc.	*	n.s.	n.s.	n.s.	n.s.	n.s.	n.s.	*	n.s.	n.s.	n.s.	n.s.	n.s.	n.s.	n.s.	n.s.
in-air avg. Y speed	n.s.	n.s.	n.s.	n.s.	n.s.	**	*	n.s.	n.s.	n.s.	n.s.	n.s.	n.s.	n.s.	*	n.s.
in-air amp Y speed	*	n.s.	n.s.	n.s.	n.s.	*	n.s.	n.s.	n.s.	n.s.	n.s.	n.s.	n.s.	n.s.	*	n.s.
in-air avg. Y acc.	*	n.s.	n.s.	n.s.	n.s.	***	n.s.	n.s.	n.s.	n.s.	n.s.	n.s.	n.s.	n.s.	*	n.s.
in-air std Y acc.	*	n.s.	n.s.	n.s.	n.s.	*	n.s.	n.s.	n.s.	n.s.	n.s.	n.s.	n.s.	n.s.	*	n.s.
in-air amp Y acc.	**	n.s.	n.s.	n.s.	n.s.	*	n.s.	n.s.	n.s.	n.s.	n.s.	n.s.	n.s.	n.s.	*	n.s.
in-air avg. speed	****	n.s.	n.s.	n.s.	n.s.	**	n.s.	n.s.	n.s.	n.s.	n.s.	*	n.s.	n.s.	*	n.s.
in-air std speed	****	n.s.	n.s.	n.s.	n.s.	n.s.	n.s.	n.s.	n.s.	n.s.	n.s.	*	n.s.	n.s.	*	n.s.
in-air amp speed	****	n.s.	n.s.	n.s.	n.s.	n.s.	n.s.	n.s.	n.s.	n.s.	n.s.	*	n.s.	n.s.	*	n.s.
in-air avg. acc.	****	n.s.	n.s.	n.s.	n.s.	*	n.s.	n.s.	n.s.	n.s.	n.s.	*	n.s.	n.s.	*	n.s.
in-air std acc.	****	n.s.	n.s.	n.s.	n.s.	n.s.	n.s.	n.s.	n.s.	n.s.	n.s.	*	n.s.	n.s.	*	n.s.
in-air amp acc.	****	n.s.	n.s.	n.s.	n.s.	n.s.	n.s.	n.s.	n.s.	n.s.	n.s.	*	n.s.	n.s.	*	n.s.
in-air std angular speed	**	n.s.	n.s.	n.s.	n.s.	n.s.	n.s.	n.s.	n.s.	n.s.	n.s.	*	n.s.	n.s.	n.s.	n.s.
in-air avg. angular speed	**	n.s.	n.s.	n.s.	n.s.	n.s.	*	n.s.	n.s.	n.s.	n.s.	*	n.s.	n.s.	*	n.s.
in-air std angular acc.	**	n.s.	n.s.	n.s.	n.s.	n.s.	n.s.	n.s.	n.s.	n.s.	n.s.	*	n.s.	n.s.	n.s.	n.s.
in-air avg. angular acc.	**	n.s.	n.s.	n.s.	n.s.	n.s.	*	n.s.	n.s.	n.s.	n.s.	*	n.s.	n.s.	n.s.	n.s.
in-air shannon entropy	****	n.s.	n.s.	n.s.	n.s.	n.s.	*	n.s.	n.s.	n.s.	n.s.	*	n.s.	n.s.	*	n.s.
on-tablet duration	***	n.s.	n.s.	**	n.s.	n.s.	*	n.s.	n.s.	n.s.	n.s.	n.s.	n.s.	n.s.	**	n.s.
on-tablet avg. X speed	**	n.s.	n.s.	n.s.	*	*	n.s.	n.s.	n.s.	n.s.	n.s.	n.s.	n.s.	n.s.	*	n.s.
on-tablet std X speed	**	n.s.	n.s.	n.s.	*	*	n.s.	n.s.	*	n.s.	n.s.	*	n.s.	n.s.	n.s.	n.s.
on-tablet amp X speed	n.s.	n.s.	n.s.	**	n.s.	n.s.	**	**	n.s.	n.s.	*	n.s.	n.s.	n.s.	n.s.	n.s.
on-tablet avg. X acc.	n.s.	n.s.	n.s.	*	*	*	n.s.	n.s.	n.s.	n.s.	*	n.s.	n.s.	*	n.s.	n.s.
on-tablet std X acc.	n.s.	n.s.	n.s.	*	n.s.	n.s.	**	*	n.s.	n.s.	*	n.s.	n.s.	n.s.	*	n.s.
on-tablet amp X acc.	n.s.	n.s.	n.s.	n.s.	*	n.s.	n.s.	**	n.s.	n.s.	*	n.s.	n.s.	n.s.	n.s.	n.s.
on-tablet avg. Y speed	n.s.	n.s.	n.s.	n.s.	*	*	n.s.	n.s.	n.s.	n.s.	n.s.	n.s.	n.s.	n.s.	n.s.	n.s.
on-tablet std Y speed	*	n.s.	n.s.	n.s.	*	*	n.s.	*	n.s.	n.s.	n.s.	n.s.	n.s.	n.s.	n.s.	n.s.
on-tablet amp Y speed	n.s.	n.s.	n.s.	n.s.	*	n.s.	*	*	n.s.	n.s.	n.s.	n.s.	n.s.	n.s.	n.s.	n.s.
on-tablet avg. Y acc.	n.s.	n.s.	n.s.	n.s.	*	n.s.	*	n.s.	n.s.	n.s.	*	n.s.	n.s.	n.s.	*	n.s.
on-tablet std Y acc.	n.s.	n.s.	n.s.	n.s.	**	n.s.	n.s.	**	n.s.	n.s.	n.s.	n.s.	n.s.	n.s.	n.s.	n.s.
on-tablet amp Y acc.	n.s.	n.s.	n.s.	n.s.	**	n.s.	n.s.	**	n.s.	n.s.	n.s.	n.s.	n.s.	n.s.	n.s.	n.s.
on-tablet avg. speed	n.s.	n.s.	n.s.	n.s.	****	*	*	n.s.	**	n.s.	*	n.s.	n.s.	n.s.	*	n.s.
on-tablet std speed	n.s.	n.s.	n.s.	n.s.	**	n.s.	*	*	n.s.	n.s.	*	n.s.	n.s.	n.s.	*	n.s.
on-tablet amp speed	*	n.s.	n.s.	n.s.	**	n.s.	n.s.	*	n.s.	n.s.	n.s.	n.s.	n.s.	n.s.	*	n.s.
on-tablet avg. acc.	n.s.	n.s.	n.s.	n.s.	****	n.s.	*	*	n.s.	n.s.	n.s.	n.s.	n.s.	n.s.	*	n.s.
on-tablet std acc.	n.s.	n.s.	n.s.	n.s.	**	n.s.	n.s.	*	n.s.	n.s.	*	n.s.	n.s.	*	n.s.	n.s.
on-tablet amp acc.	n.s.	n.s.	n.s.	n.s.	**	n.s.	n.s.	**	n.s.	n.s.	n.s.	n.s.	n.s.	*	n.s.	n.s.
on-tablet std angular speed	*	n.s.	n.s.	n.s.	**	n.s.	n.s.	n.s.	n.s.	n.s.	n.s.	n.s.	n.s.	n.s.	n.s.	n.s.
on-tablet avg. angular speed	****	n.s.	n.s.	n.s.	n.s.	n.s.	n.s.	n.s.	n.s.	n.s.	n.s.	n.s.	n.s.	n.s.	n.s.	n.s.
on-tablet std angular acc.	n.s.	n.s.	n.s.	n.s.	**	n.s.	n.s.	*	n.s.	n.s.	n.s.	n.s.	n.s.	n.s.	n.s.	n.s.
on-tablet avg. angular acc.	n.s.	n.s.	n.s.	n.s.	**	n.s.	n.s.	n.s.	n.s.	n.s.	n.s.	n.s.	n.s.	**	n.s.	n.s.
on-tablet avg. dP/dt	n.s.	n.s.	n.s.	n.s.	*	n.s.	*	n.s.	n.s.	n.s.	*	n.s.	*	*	**	n.s.
on-tablet std dP/dt	n.s.	n.s.	n.s.	n.s.	**	n.s.	*	n.s.	n.s.	n.s.	*	n.s.	*	*	*	n.s.
on-tablet amp dP/dt	n.s.	n.s.	n.s.	n.s.	**	n.s.	n.s.	*	n.s.	n.s.	n.s.	n.s.	n.s.	n.s.	n.s.	n.s.
on-tablet avg. d2P/dt2	n.s.	n.s.	n.s.	n.s.	**	n.s.	*	n.s.	n.s.	n.s.	n.s.	*	n.s.	*	*	n.s.
on-tablet std d2P/dt2	n.s.	n.s.	n.s.	n.s.	**	n.s.	*	n.s.	n.s.	n.s.	n.s.	*	n.s.	*	*	n.s.
on-tablet amp d2P/dt2	n.s.	n.s.	n.s.	n.s.	**	n.s.	n.s.	*	n.s.	n.s.	n.s.	*	n.s.	*	*	n.s.
on-tablet shannon entropy	***	n.s.	n.s.	**	*	n.s.	n.s.	n.s.	n.s.	n.s.	n.s.	n.s.	n.s.	n.s.	n.s.	n.s.

TABLE XII

TABLE OF CLASSIFICATION PERFORMANCES FOR THE RANDOM FOREST AND MULTI LAYER PERCEPTRON CLASSIFIERS.

Task	AD vs PD			PD vs PDM			AD vs CTL			AD vs PDM			PD vs CTL			PDM vs CTL		
	ACC	F1	AUC	ACC	F1	AUC	ACC	F1	AUC	ACC	F1	AUC	ACC	F1	AUC	ACC	F1	AUC
Random Forest																		
Copy Cube	64	63	73	53	52	58	63	64	70	67	65	69	64	63	66	65	62	55
Copy Image	83	83	89	53	46	62	79	79	84	78	78	80	52	52	49	58	55	64
Copy Image Memory	77	77	82	57	55	56	62	62	60	64	64	65	<b>69</b>	<b>69</b>	<b>75</b>	62	59	50
Copy Read Text	72	71	78	57	56	54	63	63	70	79	78	<b>82</b>	65	63	66	67	64	79
Copy Text	82	82	90	<b>77</b>	<b>76</b>	<b>77</b>	79	79	85	77	75	<b>81</b>	61	61	61	64	60	64
Draw Clock	78	77	88	50	49	52	77	78	88	79	78	68	60	60	56	64	64	67
Freewrite	73	73	73	59	56	70	71	71	77	79	79	78	59	58	55	75	74	<b>79</b>
Numbers	66	65	70	57	49	46	68	68	73	51	47	48	50	50	52	57	50	55
Point Dominant	88	88	93	43	41	39	83	82	84	82	82	80	62	62	62	59	57	53
Point Non-Dominant	88	88	<b>95</b>	65	64	56	<b>84</b>	<b>83</b>	89	78	76	73	68	68	71	67	66	67
Point Sustained	<b>89</b>	<b>89</b>	93	63	59	51	<b>81</b>	<b>81</b>	<b>90</b>	<b>83</b>	<b>82</b>	79	65	65	66	62	62	57
Spiral Dominant	72	71	71	60	55	56	68	68	68	73	70	58	49	48	56	69	67	64
Spiral Non-Dominant	63	62	63	68	67	68	70	69	63	75	74	67	45	43	41	64	62	59
Spiral PaTaKa	68	66	69	66	65	46	58	57	52	73	71	71	60	59	62	<b>79</b>	<b>78</b>	69
Multi Layer Perceptron																		
Copy Cube	78	78	81	53	51	52	56	56	57	69	69	69	57	57	59	52	53	51
Copy Image	84	84	90	67	63	56	72	72	82	69	68	67	59	59	62	49	48	48
Copy Image Memory	65	64	76	57	56	59	55	55	51	56	56	66	57	57	64	56	57	51
Copy Read Text	65	63	66	32	33	33	66	66	73	78	77	87	61	59	60	69	66	<b>79</b>
Copy Text	77	78	84	65	63	69	73	73	78	<b>86</b>	<b>85</b>	<b>92</b>	58	58	62	71	71	66
Draw Clock	73	72	79	59	59	51	79	79	<b>88</b>	77	76	69	54	54	61	52	53	50
Freewrite	60	59	63	59	56	50	62	62	72	75	75	77	45	45	44	73	72	75
Numbers	46	46	44	39	38	40	56	56	70	45	45	62	41	41	46	57	55	53
Point Dominant	<b>88</b>	<b>88</b>	<b>92</b>	57	53	57	81	81	84	74	71	75	62	62	<b>73</b>	64	62	65
Point Non-Dominant	83	83	89	57	55	57	84	83	82	75	72	72	59	58	68	64	64	65
Point Sustained	<b>88</b>	<b>88</b>	91	65	63	<b>67</b>	<b>87</b>	<b>87</b>	85	<b>81</b>	<b>81</b>	<b>80</b>	<b>65</b>	<b>65</b>	68	65	64	59
Spiral Dominant	67	66	74	47	42	38	59	58	58	78	75	51	56	56	55	74	74	64
Spiral Non-Dominant	61	59	60	<b>75</b>	<b>73</b>	59	69	68	69	73	66	70	48	48	49	57	51	52
Spiral PaTaKa	66	66	67	70	70	54	50	50	52	79	77	71	58	58	52	<b>77</b>	<b>76</b>	71